A New Algorithm for Multiphase-Fluid Characterization for Solvent Injection

Ashutosh Kumar, University of Alberta, and **Ryosuke Okuno,** University of Texas at Austin

Summary

Compositional simulation of solvent injection requires reliable characterization of reservoir fluids by use of an equation of state (EOS). Under the uncertainty associated with nonidentifiable components, reservoir fluids are conventionally characterized in the absence of universal methodology. This is true even for relatively simple fluids involving only the gaseous (V) and oleic (L_1) phases. No systematic method has been presented for characterization of more-complex fluids, exhibiting three hydrocarbon phases: the V, L_1, and solvent-rich-liquid (L_2) phases.

This paper presents a new algorithm for systematic characterization of multiphase behavior for solvent-injection simulation. The reliability of the method comes mainly from the binary-interaction parameters (BIPs) newly developed for the Peng-Robinson (PR) (Peng and Robinson 1976, 1978) EOS to represent three-phase behavior, including upper critical endpoints, for *n*-alkane and carbon dioxide (CO_2)/*n*-alkane binaries. The regression part in fluid characterization broadly follows the concept of perturbation from *n*-alkanes, which was successfully applied for simpler two-phase fluids in our prior research. The algorithm, in its simplest form, uses only the saturation pressure and liquid density at a given composition and reservoir temperature.

Case studies are presented to demonstrate the reliability of the algorithm for 90 reservoir fluids and their mixtures with solvents. Predictions are compared with experimental data for up to three phases. Results show that the simple algorithm developed in this research enables the PR-EOS to predict multiphase behavior in spite of the limited data used in the regression. Without the use of the BIPs developed in this research, the PR-EOS may fail to predict three phases, or may provide erroneous three-phase predictions.

Introduction

Solvent injection has been successfully implemented for enhanced oil recovery in the western United States (Mizenko 1992; Stein et al. 1992; Tanner et al. 1992; Fulco 1999; McGuire et al. 2001), Canada (Malik and Islam 2000), and the North Sea (Varotsis et al. 1986). Field pilot tests were also reported for coinjection of solvent with steam for bitumen recovery in Canada (Gupta et al. 2005; Gupta and Gittins 2006; Dickson et al. 2011).

Solvent injection can involve complex phase behavior, which consists of three hydrocarbon phases: the oleic (L_1), gaseous (V), and solvent-rich-liquid (L_2) phases. Such phase behavior has been reported for various mixtures in the literature. For binary mixtures, CO_2, methane, ethane, and propane were studied as the solvent component mixed with a heavier *n*-alkane component (Rodrigues and Kohn 1967; Kukarni et al. 1974; Hottovy et al. 1981a; Enick et al. 1985; Fall and Luks 1985; Fall et al. 1985; Estrera and Luks 1987; Peters et al. 1987a, 1987b, 1989; Van der Steen et al. 1989; Secuianu et al. 2007). Ternary mixtures were studied by Horn and Kobayashi (1967), Hottovy et al. (1981b), Hottovy et al. (1982), Llave et al. (1987), Jangkamolkulchai and Luks (1989), and Gregorowicz et al. (1993a, 1993b). Mixtures of solvents with reservoir oils were also studied by various researchers (Shelton and Yarborough 1977; Henry and Metcalfe 1983; Turek et al. 1988; Roper 1989; Sharma et al. 1989; Okuyiga 1992; Creek and Sheffield 1993; DeRuiter et al. 1994; Mohanty et al. 1995; Godbole et al. 1995).

Three-hydrocarbon-phase behavior was characterized by use of a cubic EOS for specific solvent-injection cases (Nghiem and Li 1986; Negahban and Kremesec 1989; Sharma et al. 1989; Khan et al. 1992; Okuyiga 1992; Creek and Sheffield 1993; Reid 1994; Godbole et al. 1995; Mohanty et al. 1995; Guler et al. 2001; Aghbash and Ahmadi 2012). The EOSs used by them include the PR-EOS (Peng and Robinson 1976, 1978) and the Soave-Redlich-Kwong EOS (Soave 1972). Their results indicate that these equations are capable of correlating three-hydrocarbon-phase behavior quantitatively. However, their characterization procedures were specific to the fluids studied. No systematic knowledge has been presented of how three-hydrocarbon-phase behavior can be reliably characterized for solvent injection (Okuno and Xu 2014a).

This paper presents a new algorithm for characterization of multiphase behavior with the PR-EOS. The term "multiphase behavior" in this paper refers to volumetric and compositional behavior of equilibrium phases consisting of at most three hydrocarbon phases. Hence, the algorithm accommodates the traditional vapor/liquid-phase behavior as a subset of the research scope. The next section describes the algorithm developed. Then, case studies are presented for 90 reservoir fluids, for which experimental data are available in the literature.

Multiphase-Fluid Characterization

Fluid characterization consists of three major steps.

- Step 1: compositional characterization of the plus fraction
- Step 2: initial estimates for components' properties, such as critical temperature (T_C), critical pressure (P_C), and acentric factor (ω)
- Step 3: regression to the pressure/volume/temperature (PVT) data available

The current research uses the method of Quiñones-Cisneros et al. (2004) for Step 1.

Steps 2 and 3 broadly follow the methodology of Kumar and Okuno (2013), which is referred to as perturbation from *n*-alkanes (PnA). In the PnA method, Step 2 assumes that pseudocomponents are *n*-alkanes; that is, they are assigned T_C, P_C, and ω of equivalent *n*-alkanes in terms of carbon number (CN). Then, Step 3 systematically adjusts the properties of all pseudocomponents in the direction of increasing aromaticity from *n*-alkanes (i.e., zero aromaticity). In the initial stage of this research, the validity of this methodology for three phases was confirmed with the data for ternary mixtures of methane, ethane, and tetradecylbenzene given in Jangkamolkulchai and Luks (1989).

In Step 2 of Kumar and Okuno (2013, 2015), the *n*-alkane properties were taken from Kumar and Okuno (2012), in which T_C, P_C, and ω of *n*-alkanes were optimized for the PR-EOS to accurately predict vapor pressure and liquid density. Hence, the PR-EOS was initially calibrated with vapor pressure and liquid density of *n*-alkanes before characterizing reservoir fluid. For the current research, however, Step 2 requires that the PR-EOS be calibrated with binary three-phase behavior. Therefore, BIPs have been optimized for the PR-EOS to represent binary three-phase data taken from the literature, such as those for CO_2, methane, ethane, and propane with heavier *n*-alkanes (Appendix A). This BIP optimization was conducted by use of the Gao et al. (2001) correlations for T_C and P_C:

This paper (SPE 175123) was accepted for presentation at the SPE Annual Technical Conference and Exhibition, Houston, 28–30 September 2015, and revised for publication. Original manuscript received for review 8 September 2015. Revised manuscript received for review 6 March 2016. Paper peer approved 8 March 2016.

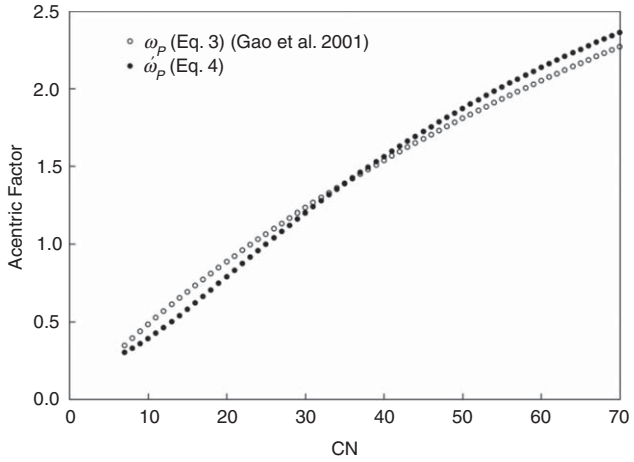

Fig. 1—Comparison of physical ω (Eq. 3) with $\acute{\omega}$ (Eq. 4) that can be used to match the UCEP data with the PR-EOS.

$$T_{CP} = \{6573.87 - 4680.77 \times \exp[-0.1831(CN^{0.6667} - 2.08)]\}^{\frac{1}{1.276}}, \quad \ldots\ldots (1)$$

$$P_{CP} = 42.44\exp[-0.3757(CN^{0.5684} - 1.8672)], \quad \ldots\ldots (2)$$

for *n*-alkanes (or paraffins) heavier than hexane. Gao et al. (2001) also presented a correlation for ω for *n*-alkanes:

$$\omega_P = \{3.212102 - 2.937628 \times \exp[-0.04699(CN^{0.6667} - 2.08)]\}^{\frac{1}{0.6851}}. \quad \ldots\ldots (3)$$

As discussed in Appendix A, however, the following correlation has been found to perform better for the BIP optimization in this research:

$$\acute{\omega}_P = 0.217066 + 5.27405CN^{-\left(\frac{14.8147}{CN}\right)}. \quad \ldots\ldots (4)$$

The deviation of Eq. 4 from Eq. 3 is minor, as presented in **Fig. 1.**

Eqs. 1 and 2 are used for the initialization of pseudocomponents in Step 2. The initial values for ω are all zero for the pseudocomponents.

In Step 3, the properties for all pseudocomponents are systematically perturbed from the initial values until the saturation pressure at the reservoir temperature is matched. They are perturbed monotonically in the increasing direction. The monotonic, systematic increases of T_C, P_C, and ω require certain trends with respect to CN, which represent the effect of aromaticity on vapor-pressure curves of pseudocomponents. For this purpose, higher values have been empirically determined for T_C, P_C, and ω for a nonzero aromaticity, as follows:

$$T_{CH} = 5339.14 - 4850.41\exp^{(-0.0016507276 69CN^{1.4223})}, \quad \ldots. (5)$$

$$P_{CH} = 48.0823 - 21.7852\exp^{(-11.372937CN^{-1.326532})}, \quad \ldots\ldots (6)$$

$$\omega_H = 0.026547(0.985567^{CN})(CN^{1.295419}). \quad \ldots\ldots (7)$$

These correlations are determined on the basis of phase-behavior data for a wide range of fluid types, such as gas condensate, volatile oil, and heavy oil, to cover a wide CN range. The data used include constant volume depletion (CVD), slimtube minimum miscibility pressure (MMP), and swelling test. Eqs. 5 through 7 represent the trend of vapor-pressure curves with a certain level of aromaticity. Although they are empirical within this research, these equations have been confirmed to be quantitatively reasonable by comparing with measured T_C, P_C, and ω for aromatics given in Yaws (2010) and Nikitin and Popov (2015).

BIPs are not adjusted in Step 3. As given in Appendix A, correlations have been developed for BIPs for CO_2, methane, ethane, and propane:

$$K_{CO_2} = (-24.7255 + 0.1412CN^{2.7213})/(663.288 + CN^{2.7213}), \quad \ldots\ldots (8)$$

$$K_{methane} = 0.0428 + 0.0009CN, \quad \ldots\ldots (9)$$

$$K_{ethane} = 0.0405 + 0.00011CN, \quad \ldots\ldots (10)$$

$$K_{propane} = 0.07419 - 0.04326\exp^{(-0.00013754CN^{2.518052})}, \quad \ldots\ldots (11)$$

for $CN > 6$. Extrapolation of the BIPs for methane, ethane, and propane has yielded the following correlations for butane and pentane:

$$K_{butane} = 0.11\left(0.000133426^{\frac{1.0}{CN}}\right)CN^{-0.0324628}, \quad \ldots\ldots (12)$$

$$K_{pentane} = 0.13\exp^{\left(-\frac{15.5385}{CN}\right)}. \quad \ldots\ldots (13)$$

The developed algorithm is presented here.

Step 1: Compositional Characterization. The plus fraction for the fluid of interest is split into the user-specified number (*n*) of pseudocomponents with a chi-squared distribution (Quiñones-Cisneros et al. 2004).

Step 2: Deviation in Saturation Pressure. The initial deviation in saturation pressure is calculated as the ratio of the measured saturation pressure (P_S) to the calculated saturation pressure (P_{S_EOS}) by use of the PR-EOS with Eqs. 1, 2, and 4. The ratio is denoted as β.

Step 3: Incremental Values for T_C, P_C, and ω. Incremental values for T_C, P_C, and ω during the regression are determined as follows:

$$\Delta T_{C,i} = (T_{CH,i} - T_{CP,i})/(\beta N), \quad \ldots\ldots (14)$$

$$\Delta P_{C,i} = (P_{CH,i} - P_{CP,i})/N, \quad \ldots\ldots (15)$$

$$\Delta\omega_i = \omega_{H,i}/N, \quad \ldots\ldots (16)$$

for $i = 1, 2, \ldots, n$, where N is an integer to be specified by the user (e.g., $N = 10^4$, as used in this research). Set the iteration-step index k to be unity.

Step 4: Update of T_C, P_C, and ω.

$$T_{C,i} = T_{CP,i} + k\Delta T_{C,i}, \quad \ldots\ldots (17)$$

$$P_{C,i} = P_{CP,i} + k\Delta P_{C,i}, \quad \ldots\ldots (18)$$

$$\omega_i = k\Delta\omega_i. \quad \ldots\ldots (19)$$

Step 5. Convergence Test. Calculate $\delta = (P_S - P_{S\_EOS})/P_S$. Proceed to Step 6 if $|\delta| < \delta_{TOL}$ (e.g., $\delta_{TOL} = 10^{-4}$). Otherwise, return to Step 4 after increasing k by one: $k = k + 1$.

Step 6. Volume Shift. Volume-shift parameters are adjusted to match liquid-density data, as required.

Critical parameters and acentric factors are perturbed as monotonic functions of the iteration-step index k. It has been consistently observed in this research that the calculated P_S increases with increasing k during the iteration. **Fig. 2a** depicts that vapor-pressure curves for all pseudocomponents change systematically and monotonically as the iteration proceeds for an example case of a light oil. Fig. 2b shows the two-phase envelopes corresponding to the three sets of vapor-pressure curves given in Fig. 2a.

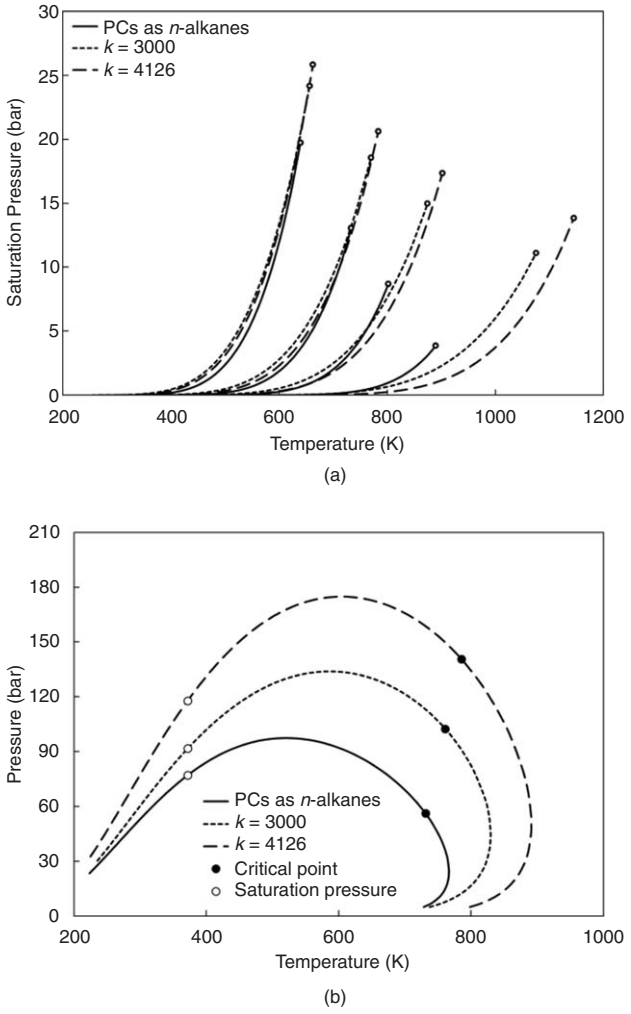

Fig. 2—(a) Systematic changes in vapor-pressure curves for pseudocomponents (PCs) and (b) the resulting PT envelopes with changing *k* index during regression. The *k* index is presented in the stepwise description of the algorithm in the Multiphase-Fluid Characterization section. This example is for a light oil with saturation pressure at 372.05 K.

Volume shift is performed to match liquid-density data only after the model is set in terms of compositional phase behavior. This is because a change in compositional-behavior prediction affects volumetric predictions, as discussed in detail by Kumar and Okuno (2013). For fluid characterization with a PnA-based approach, density data for a liquid phase that is in equilibrium with the V phase are more important than those from a single-phase fluid or equilibrium V phase (Kumar and Okuno 2015). This was confirmed also in this research. Hence, it is recommended that Step 6 use density data from an equilibrium-liquid phase.

Case Studies

The algorithm is applied to 90 reservoir fluids in this section, which are gas condensates, volatile oils, heavy oils, and bitumens. The fluids tested are characterized as 12 components, which consist of N_2, CO_2, C_1, C_2, C_3, C_4, C_5, C_6, and four pseudocomponents, by use of the PR-EOS with the van der Waals mixing rules. The regression algorithm uses only P_S and saturated-liquid-density data, as shown previously.

T_C, P_C, and ω for well-defined pure components are taken from Yaws (2010), and they are not adjusted. **Table 1** gives the BIPs used in this section. Note that BIPs are not adjusted in the regression algorithm developed. However, it is possible to adjust them individually when specific data are to be matched. T_C, P_C, and ω for pseudocomponents are adjusted to match P_S. Volume-shift parameters are adjusted to match saturated-liquid-density data at the final step of the algorithm. Then, the quality of prediction from the resulting EOS model is demonstrated with other types of data, such as three hydrocarbon phases, CVD, constant mass expansion (CME), and MMP for V/L.

***L/V* Phase Behavior.** This subsection shows results for two-phase predictions. **Table 2** lists 55 light fluids for which CVD and CME data are available in the literature. In the table, Fluids 1 through 48 are gas condensates and the others are volatile oils. The fifth, sixth, and seventh columns show the value of β, the number of iterations (i.e., k discussed previously), and the degree of freedom in the chi-squared distribution, respectively. The eighth column indicates CVD data as Data Type 1 and CME as Data Type 2. This column also indicates the limiting value from measured data. The right-most column gives the average absolute deviation (AAD), $\frac{1}{M}\sum_{j=1}^{M}|\text{Prediction} - \text{Data}|_j$, for the data type indicated for each fluid.

	N_2	CO_2	CH_4	C_2	C_3	C_4	C_5	C_6	PC-1	PC-2	PC-3	PC-4
N_2	0.0000	–	–	–	–	–	–	–	–	–	–	–
CO_2	0.0000	0.0000	–	–	–	–	–	–	–	–	–	–
CH_4	0.1000	0.1000	0.0000	–	–	–	–	–	–	–	–	–
C_2	0.1000	0.1450	0.0420	0.0000	–	–	–	–	–	–	–	–
C_3	0.1000	Kato et al. (1981)	0.0420	0.0400	0.0000	–	–	–	–	–	–	–
C_4	0.1000	Kato et al. (1981)	0.0420	0.0400	0.0300	0.0000	–	–	–	–	–	–
C_5	0.1000	Kato et al. (1981)	0.0420	0.0400	0.0300	0.0116	0.0000	–	–	–	–	–
C_6	0.1000	Kato et al. (1981)	0.0420	0.0400	0.0300	0.0155	0.0058	0.0000	–	–	–	–
PC-1	0.1300	(8)	(9)	(10)	(11)	(12)	(13)	0.0000	0.0000	–	–	–
PC-2	0.1300	(8)	(9)	(10)	(11)	(12)	(13)	0.0000	0.0000	0.0000	–	–
PC-4	0.1300	(8)	(9)	(10)	(11)	(12)	(13)	0.0000	0.0000	0.0000	0.0000	–
PC-4	0.1300	(8)	(9)	(10)	(11)	(12)	(13)	0.0000	0.0000	0.0000	0.0000	0.0000

Table 1—Binary-interaction parameters used with the new algorithm. Numbers inside parentheses indicate the corresponding equations in this paper. Eqs. 11 through 14 of Kato et al. (1981) are used. PC = pseudocomponent.

Fluid No.	References	MW (g/mol)	Reservoir Temperature (K)	β	k	p	Limiting Data Value (Type No.)	AAD
1	Al-Meshari (2004), Fluid 3	31.53	424.82	1.374	4722	2.0	11.70 (1)	0.58
2	Al-Meshari (2004), Fluid 4	31.44	403.15	1.322	4682	2.0	13.00 (1)	1.25
3	Al-Meshari (2004), Fluid 5	32.41	382.59	1.271	4764	2.1	23.36 (2)	2.38
4	Al-Meshari (2004), Fluid 7	36.62	397.59	1.493	5420	2.6	25.00 (1)	2.49
5	Al-Meshari (2004), Fluid 8	40.77	424.82	1.309	4204	2.2	30.40 (1)	4.73
6**	Al-Meshari (2004), Fluid 10	39.23	422.59	1.135	3879	3.3	33.60 (1)	0.63
7**	Al-Meshari (2004), Fluid 11	41.71	424.82	1.211	4348	3.0	32.20 (1)	2.94
8**	Coats and Smart (1986), Gas 5	30.29	403.70	1.241	4593	2.0	10.40 (2)	0.59
9	Coats and Smart (1986), Gas 2	44.92	360.92	2.334	4399	4.0	53.06(1)	1.40
10	Guo and Du (1989), Sample 7	25.53	406.45	1.310	4800	2.0	5.82 (1)	0.34
11	Metcalfe and Raby (1986)	35.70	374.82	1.230	4075	2.2	23.89 (1)	2.96
12**	Coats (1985), recombined	44.40	435.93	1.042	4340	4.0	32.00 (2)	2.34
13**	Coats (1985), bottomhole	44.40	435.93	1.085	4155	4.0	33.49 (2)	4.20
14**	McVay (1994), Gas B	40.58	387.59	1.184	3785	2.0	40.90 (1)	1.18
15	Danesh (1998)	27.29	394.00	1.443	4864	2.0	11.32 (1)	1.91
16	Pedersen and Christensen (2007)	29.14	428.15	1.453	5566	2.0	11.89 (2)	2.46
17	Hosein et al. (2013), PL-1	23.64	358.78	1.270	4591	2.0	8.15 (1)	1.12
18	Hosein et al. (2013), PL-2	22.10	378.15	1.744	6575	2.0	5.08 (1)	0.49
19	Hosein et al. (2013), PL-3	21.55	357.59	1.120	4429	2.0	4.00 (1)	0.31
20	Hosein et al. (2013), PL-4	20.62	364.22	1.490	5949	2.0	3.73 (1)	0.28
21	Hosein et al. (2013), PL-5	20.30	355.37	1.158	4806	2.0	3.79 (1)	0.30
22	Hosein et al. (2013), PL-6	19.75	367.59	1.769	7597	2.0	1.89 (1)	0.07
23	Kenyon and Behie (1987)	32.61	366.48	1.025	3956	2.5	19.90 (1)	2.61
24	Moore (1989)	24.45	365.37	1.476	7412	2.0	2.17 (1)	0.24
25	Whitson and Torp (1983), NS-1	35.04	410.43	1.390	4208	2.0	21.60 (1)	0.88
26	Whitson and Brule (2000), GOCW-7	33.62	358.70	1.304	5690	2.5	23.90 (1)	2.82
27	Drohm et al. (1988), Example 2	32.65	436.70	1.475	4643	2.0	15.63 (1)	2.61
28	Drohm et al. (1988), Example 3	26.26	393.20	1.558	6856	2.0	4.75 (1)	0.70
29	Drohm et al. (1988), Example 4	28.34	377.60	1.443	5962	2.1	11.84 (1)	1.38
30	Drohm et al. (1988), Example 5	21.27	377.60	1.868	8865	2.0	1.69 (1)	0.04
31	Akpabio et al. (2014)	26.35	377.04	1.550	5825	2.0	10.53(1)	0.45
32	Pedersen et al. (1989)*	26.98	392.10	1.694	7048	2.1	5.72 (1)	0.78
33	Vogel and Yarborough (1980), Gas 1*	36.03	381.00	1.105	3746	2.2	25.85 (2)	1.53
34	Vogel and Yarborough (1980), Gas 2*	30.75	381.00	1.194	4229	2.1	9.79 (2)	1.64

Table 2—Characterization results for gas condensates and volatile oils with the new algorithm. CVD or CCE data are available for these fluids. Parameters β and k are defined in the algorithm section of the text. Parameter p indicates the degree of freedom in the chi-squared distribution. In the Limiting Data Value column, Type No. 1 is CVD liquid saturations (%) and Type No. 2 is CCE liquid saturations (%). The AAD column is the summation of (experimental value – predicted value) divided by the number of data points.

Fluid No.	References	MW (g/mol)	Reservoir Temperature (K)	β	k	p	Limiting Data Value (Type No.)	AAD
35	Vogel and Yarborough (1980), Gas 3*	23.73	333.00	1.197	6351	2.1	3.40 (2)	0.60
36**	Whitaker and Kim (1993)	39.34	366.48	1.218	3982	2.2	47.40 (2)	7.94
37	Kilgren (1966)*	36.52	399.82	1.689	3321	2.1	39.99 (2)	5.53
38**	Subero (2009)*	40.03	377.04	1.053	4345	2.1	38.90 (1)	2.63
39	Fawumi (1999)	34.04	422.59	1.226	4205	2.1	17.16 (1)	1.97
40	Al-Subai (2001), Well A	32.64	420.93	1.254	4296	2.6	14.34 (1)	1.66
41	Al-Subai (2001), Well B	42.44	424.82	1.156	3759	2.6	32.02 (1)	2.91
42	Al-Subai (2001), Well D	34.50	424.82	1.232	4225	2.1	17.17 (1)	2.31
43	Al-Subai (2001), Well E	23.03	412.59	1.910	7907	2.1	2.18 (1)	0.28
44	Jacoby et al. (1959)	32.76	404.82	1.227	4110	2.1	16.10 (2)	0.46
45	Renner et al. (1989)	35.69	374.82	1.227	4058	2.1	25.02 (2)	0.38
46	Spivak (1971)	27.13	352.59	1.063	4408	2.1	12.68 (1)	1.32
47	Firoozabadi et al. (1978)	23.83	355.65	1.143	4940	2.0	4.70(1)	0.54
48**	Gajda (2014)	42.94	364.15	1.530	4476	2.0	49.50(1)	2.20
49	Al-Meshari (2004), Fluid 12	46.07	354.82	1.519	4039	2.3	38.20 (1)	1.80
50	Al-Meshari (2004), Fluid 16	59.63	425.93	1.342	3507	2.5	35.30 (1)	1.28
51**	McVay (1994), Oil A	50.93	408.70	1.357	4355	2.5	33.30 (1)	3.91
52	McVay (1994), Oil B	57.50	393.70	1.332	4027	3.1	49.50 (1)	1.45
53	Jacoby and Yarborough (1967)	54.32	346.48	1.343	4201	2.8	24.29 (2)	1.94
54**	Pedersen et al. (1989)	47.84	424.25	1.357	3719	2.3	42.20 (1)	4.57
55	Reudelhuber and Hinds (1957)	42.55	374.82	1.152	3548	2.3	34.50 (1)	1.57

* Density data for gas condensates Nos. 32, 33, 34, 35, 37, and 38 are not available. Density matching for these fluids has not been performed.

** Near-critical gas condensates.

Table 2 (continued)—Characterization results for gas condensates and volatile oils with the new algorithm. CVD or CCE data are available for these fluids. Parameters β and k are defined in the algorithm section of the text. Parameter p indicates the degree of freedom in the chi-squared distribution. In the Limiting Data Value column, Type No. 1 is CVD liquid saturations (%) and Type No. 2 is CCE liquid saturations (%). The AAD column is the summation of (experimental value – predicted value) divided by the number of data points.

Before performing Step 6, the AAD for saturated-liquid densities for all the fluids in Table 2 was less than 2%, indicating the accuracy of the PR-EOS for light fluids. They were eventually matched in Step 6.

The results given in Table 2 show that the new algorithm is capable of predicting CVD and CME liquid saturations well. The deviation tends to be high for near-critical fluids (Nos. 6, 7, 8, 12, 13, 14, 36, 38, 48, 51, and 54). This is because liquid saturation is sensitive to pressure near saturation pressure for those fluids. **Fig. 3** shows the CME liquid saturation for Fluid 36, which gives the highest AAD in Table 2. Fluid 54 is also a near-critical fluid. However, **Fig. 4** shows satisfactory predictions of CVD liquid saturations for this near-critical fluid.

Table 3 shows reservoir oils for which MMP data from slimtube tests are available in the literature. MMP prediction serves as a severe test for fluid characterization because it requires accurate prediction of compositional phase behavior away from the original oil composition in multicomponent composition space. Thermodynamic MMPs are calculated with the method of characteristics within PVTsim (Calsep 2012), and compared with data. The calculated MMPs likely correspond to the *V*/*L* miscibility, considering their reservoir temperatures and that PVTsim did not indicate any difficulty associated with three phases in the calculations. The average absolute relative deviation (AARD), $\frac{1}{M}\sum_{j=1}^{M}\left|\frac{\text{Prediction}-\text{Data}}{\text{Data}}\right|_j$, for all 26 MMP predictions is 4.57%. Some level of deviation of thermodynamic MMP from slimtube MMP is inevitable because of the presence of dispersion in real displacement of oil by gas. However, the present algorithm shows improved MMP predictions, because the AARDs with earlier characterizations were 6.7% (Kumar and Okuno 2013) and 6.4% (Kumar and Okuno 2015).

The algorithm was also tested in terms of other types of phase behavior. **Table 4** lists heavy oils for which swelling-test (ST) data, gas/oil ratio (GOR), and *V*/*L* boundary in pressure/temperature (PT) space are available in the literature. Oil 1 in Table 4 is West Sak oil (Sharma 1990), for which the AARD in GOR prediction is 7%.

ST data are available for Oil 2 with a gas mixture of 14% CO_2, 17% methane, 60% ethane, 4% propane, 3% butane, and 2% pentane (Krejbjerg and Pedersen 2006). The saturation pressures for different gas/oil mixing ratios were predicted satisfactorily, as shown in **Fig. 5.** The AARD for the predictions is 3.4%. Pedersen et al. (2004) showed GOR data for Oil 3, for which the PR-EOS model with the current characterization algorithm gives an AARD

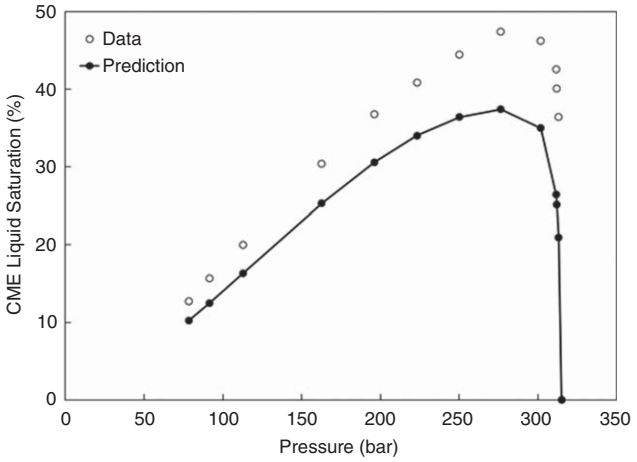

Fig. 3—CME liquid saturation predicted for near-critical gas condensate, Fluid 36 in Table 2, at 366.48 K. The molecular weight is 39.34 g/mol. The mole fraction and molecular weight of the heptane plus are 0.1003 and 172.0 g/mol, respectively.

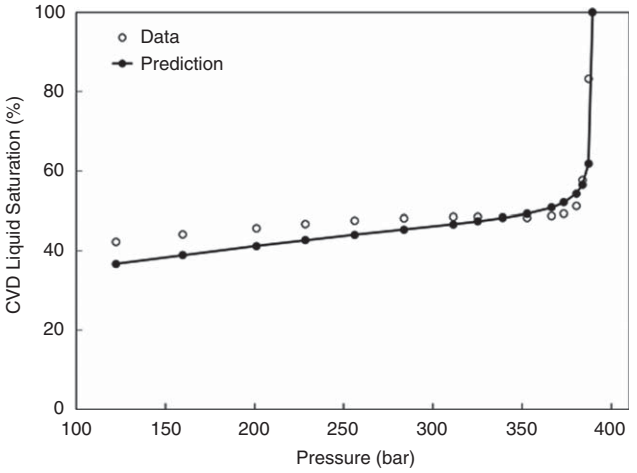

Fig. 4—CVD liquid saturation predicted for near-critical volatile oil, Fluid 54 in Table 2, at 424.25 K. The molecular weight is 47.84 g/mol. The mole fraction and molecular weight of the heptane plus are 0.1417 and 194.0 g/mol, respectively. The critical point was measured at 426 K and 388 bar. The critical point predicted with the characterized EOS is at 434.65 K and 391.43 bar.

of 4.42%. As shown in **Fig. 6,** the GOR predictions are in good agreement with the data.

PVT data for Lloydminster heavy oil were presented in Li et al. (2013a) (Oil 4 in Table 4). The dead-oil composition was characterized with four pseudocomponents on the basis of the chi-squired distribution with a degree of freedom of nine. The saturation pressure of 56.64 bar at 347.67 K for Feed No. 5 (31.7% CO_2, 34.3% butane, and 0.34% heavy oil) was used for characterization with the new algorithm. The characterized oil was then used to predict the saturation pressure for Feed No. 4 (38.6% CO_2, 36.2% propane, and 25.2% heavy oil). **Fig. 7** shows that the predictions are close to the reported data, yielding an AARD of 5.60% for the seven data points.

***L*/*L*/*V* Phase Behavior.** In this subsection, the new algorithm with the developed BIPs is tested by comparing three-phase-behavior predictions with experimental data. Note that the algorithm matches only P_S at the oil composition as far as compositional phase behavior is concerned; i.e., no parameter is adjusted for matching three-phase data for oil/solvent mixtures to be presented here.

To show the importance of the BIPs developed in this research, this subsection also presents phase-behavior predictions when the algorithm is used with two conventional sets of BIPs. In one of the conventional sets, BIPs are zero for all hydrocarbon/hydrocarbon pairs and 0.1 for CO_2 with pseudocomponents (Peng and Robinson 1978). These BIPs are often used for *V*/*L*-phase-behavior representation, which is simpler than three-phase representation. All other BIPs are presented in Table 1.

In the other conventional set, BIPs for methane, ethane, and propane with pseudocomponents are 0.04, 0.01, and 0.01, respectively, on the basis of Peng and Robinson (1978). All other BIPs are presented in Table 1.

Three sets of BIPs are compared with experimental data in this section. Predictions with the BIPs developed in this research are shown as "new BIPs." Those with the two conventional BIPs are shown as "zero BIPs" and "PR BIPs."

Three-phase data are available for Oils 1, 4, 5, and 6 from Table 4. Three phases were reported for the mixture of 20% of Oil 1 and 80% of CO_2 at 299.81 K. **Fig. 8** compares predicted saturations for the L_1 (Fig. 8a) and L_2 (Fig. 8b) phases with experimental data. The AARD for the L_1-phase saturations is 5.61%. With the new algorithm, the PR-EOS correctly predicts the presence of three phases for this mixture; i.e., they were experimentally observed between 77.20 and 83.75 bar, and predicted between 76.46 and 82.47 bar. The characterization with zero hydrocarbon/hydrocarbon BIPs shows the presence of three phases in a relatively small pressure range (79.21–83.0 bar), as can be seen in Fig. 8b. The PR-BIPs case gives similar saturations to those in the zero-BIPs case, mainly because the same BIPs are used for CO_2 with hydrocarbons.

Fig. 9 shows phase boundaries between two and three phases in PT space for Feeds Nos. 14 (Fig. 9a) and 15 (Fig. 9b) with Oil 4 in Table 4. Feed No. 14 is 23.6% propane, 67.2% CO_2, and 9.2% oil, and Feed No. 15 is 11.8% butane, 83.2% CO_2, and 5.0% oil. The results show that the PR-EOS models with the new characterization algorithm give satisfactory predictions for these complex mixtures. This also validates the reliability of the BIP correlation (Eq. 12) for butane, which was developed by extrapolation of BIP values for methane, ethane, and propane. However, the characterization with zero hydrocarbon/hydrocarbon BIPs shows a narrow three-phase region near the *LL*/*LLV* boundary. The PR-BIPs case predicts the presence of three phases for both feeds, but the deviation from data is greater than when the new BIPs are used.

Oil 5 given in Table 4 is Athabasca bitumen, for which Badamchi-Zadeh et al. (2009) presented three-phase data. The dead-oil composition was characterized with four pseudocomponents on the basis of the chi-squired distribution with a degree of freedom of 12. The algorithm was applied with the saturation pressure, 10.82 bar, reported for a mixture of 59.3% bitumen with 40.7% propane at 333.15 K. The resulting fluid model was then used to predict three-phase behavior for the mixture of 51.0% CO_2, 34.7% propane, and 14.3% bitumen. **Fig. 10** shows satisfactory predictions of phase boundaries in spite of the large amount of CO_2 present in the predicted mixture. The characterization with zero hydrocarbon/hydrocarbon BIPs results in a larger three-phase region. The PR-BIPs case also results in a large deviation from the data.

Oil 6 given in Table 4 is Peace River bitumen. The molecular weight (MW) used in the characterization is 527.5 g/mol, according to Mehrotra and Svrcek (1985). This bitumen was characterized by use of the saturation pressure, 50.50 bar, reported by Mehrotra and Svrcek (1985) for a mixture of 21.83% methane and 78.17% bitumen at 326.65 K. The resulting fluid model was then used to predict three phases in PT space for another mixture, of 89.94% pentane and 10.06% bitumen. The predicted three-phase behavior was compared with three-phase behavior for this mixture composition simulated by Agrawal (2012). **Fig. 11** presents that the predicted three-phase region is narrower than in Agrawal (2012) in PT space. The difference is inevitable because of the lack of comprehensive data; i.e., the bitumen MW in the characterization by Agrawal (2012) was 580 g/mol. Nevertheless, the successful prediction of three phases indicates the validity of the BIP correlation (Eq. 13) for pentane, which was developed by

Oil No.	References	MW (g/mol)	Reservoir Temperature (K)	β	k	p	AARD MMP Prediction (%)
1	Jaubert et al. (2002), F1	135.24	374.85	1.329	3413	4.5	2.76
2	Jaubert et al. (2002), F2	136.25	372.05	1.528	4126	4.7	13.19
3	Jaubert et al. (2002), F3	82.41	387.35	1.437	4044	6.3	0.91
4	Jaubert et al. (2002), F4	63.17	388.20	1.387	3883	3.0	3.17
5	Jaubert et al. (2002), F5	125.82	394.25	1.520	4063	4.5	2.29
6	Jaubert et al. (2002), F6	96.25	383.15	1.324	3731	4.2	3.27
7	Jaubert et al. (2002), F7	96.19	393.15	1.317	4181	4.9	3.17
8	Jaubert et al. (2002), F11	82.55	373.75	1.401	3947	3.8	6.47
9	Ekundayo (2012)	86.57	402.59	1.331	4142	4.6	0.94
10	Høier (1997)*						
	Injection gas (System 1)**	97.0	368.15	1.550	4160	4.4	12.35
	Injection gas (System 2)**	97.0	368.15	1.550	4160	4.4	6.03
	Injection gas (System 3)**	97.0	368.15	1.550	4160	4.4	6.70
	Injection gas (System 4)**	97.0	368.15	1.550	4160	4.4	8.53
11	Graue and Zana (1981)†	177.0	344.26	1.493	4874	7.7	7.38
	Graue and Zana (1981)†	177.0	344.26	1.493	4874	7.7	9.62
12	Negahban et al. (2010)	101.90	394.00	1.276	3812	4.8	1.96
13	Firoozabadi and Khalid (1986), XA	51.58	444.26	1.289	3793	3.1	0.30
14	Firoozabadi and Khalid (1986), XB	67.33	366.48	1.519	4240	3.4	1.46
15	Firoozabadi and Khalid (1986), XC	86.25	380.37	1.768	4089	3.2	0.42
16	Firoozabadi and Khalid (1986), XD	89.07	423.71	1.650	3974	3.3	3.32
17	Lee and Reitzel (1982), A	78.35	376.15	1.318	4238	4.5	2.26
18	Lee and Reitzel (1982), D	79.85	375.15	1.278	3821	4.1	8.64
19	Lee and Reitzel (1982), E	54.33	379.15	1.358	4193	3.2	3.40
20	Koch and Hutchinson (1958), A						
	Injection gas 1	64.97	333.15	1.364	4604	3.1	7.02
	Injection gas 2	64.97	333.15	1.364	4604	3.1	1.73
	Injection gas 3	64.97	333.15	1.364	4604	3.1	2.75
	Injection gas 4	64.97	333.15	1.364	4604	3.1	3.53

*Simulated MMPs

** Oil composition (System VOA) and saturation data used were taken from Whitson and Belery (1994). Systems 1 through 4 indicate four different injection gases. The MMPs reported were simulated.

† Two different injection gases have been used. Further details are available in Graue and Zana (1981).

Table 3—Characterization results for oils for which slimtube MMP data are available. Parameters β and k are defined in the algorithm section. Parameter p indicates the degree of freedom in the chi-squared distribution.

extrapolation of BIP values for methane, ethane, and propane. However, no three-phase region was predicted by the characterization with the zero-BIPs and PR-BIPs cases.

Table 5 lists reservoir oils for which three phases with CO_2 were reported in the literature. Results show that the new algorithm gives reasonable predictions for these fluids. As an example, **Fig. 12** presents phase boundaries in pressure-composition (P-x) space space for Oil C2 with CO_2 at 313.71 K, for which the data were taken from Turek et al. (1988). Although the EOS gives higher immiscibility than the data in Fig. 11, their agreement is remarkable considering that only P_S and liquid-density data at the oil composition were used in the characterization. Also, the regression was conducted only for T_C, P_C, and ω of pseudocomponents; i.e., the effect of oil aromaticity on the interaction between oil and CO_2 was not explicitly considered in the algorithm.

The oils listed in Table 5 were also characterized for the zero-BIPs and PR-BIPs cases, to see the importance of the BIPs developed in this research. Out of the nine oils, the presence of three phases was predicted for only three oils (Oil Nos. 6, 8, and 9) with the two conventional sets of BIPs. Fig. 12 shows that the

Oil No.	References	MW (g/mol)	Temperature (K)	β	k	p	AARD (%)	Type of Data
1**	Sharma (1990), West Sak Oil	228.88	299.81	1.783	3350	5.7	3.45*	ST
2	Krejbjerg and Pedersen (2006), Fluid 1	125.72	347.15	1.705	4269	5.5	3.40	ST
3	Pedersen et al. (2004), Fluid 22	311.06	305.45	2.291	3587	5.5	4.42	GOR
4**	Li et al. (2013a), Lloydminster Oil	482.00	347.67	1.352	3166	9.0	5.60	PT
5**	Badamchi-Zadeh et al. (2009), Athabasca bitumen	552.00	333.15	1.060	2870	12.0	–	PT
6**	Mehrotra and Svrcek (1985), Peace River bitumen	527.50	326.65	1.541	2625	12.0	–	PT

* Includes oleic-phase saturation prediction for 60% and 80% CO_2 mixtures. For 60% CO_2 mixture only, it is 1.53%.

** For Oils 1, 4, 5, and 6, three-phase pressure/temperature envelopes are shown in separate figures in the *L/L/V* Phase Behavior subsection, and two-phase predictions are shown in separate figures in the *L/V* Phase Behavior subsection.

Table 4—Characterization results for heavy oils and bitumens with the new algorithm. PVT data for these oils include STs, gas solubility, and phase envelopes. Parameters β and k are defined in the algorithm section. Parameter p indicates the degree of freedom in the chi-squared distribution. PT = two-phase and three-phase pressure/temperature data.

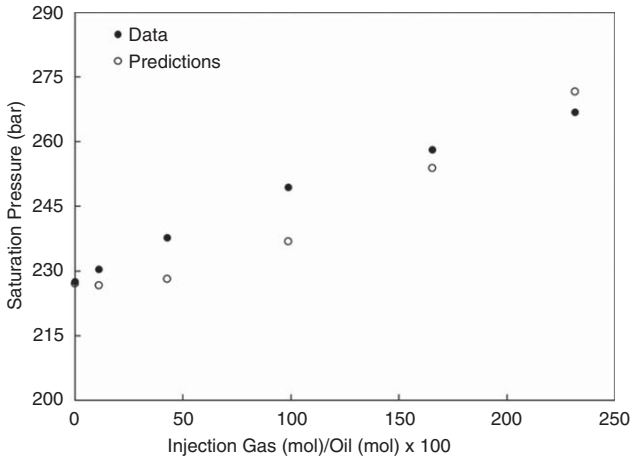

Fig. 5—Saturation pressures during the swelling test for Oil 2 in Table 4 at 347.15 K. The molecular weight and °API value of the oil are 125.98 g/mol and 28, respectively.

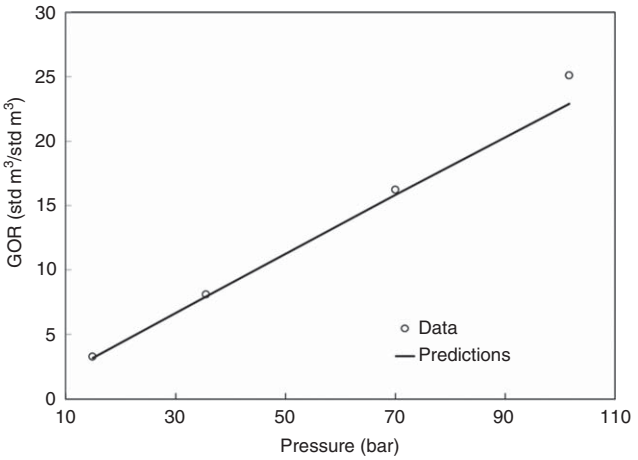

Fig. 6—GOR predictions at 305.45 K for Oil 3 in Table 4. The molecular weight of Oil 3 is 311.06 g/mol. This is a highly aromatic oil, according to Pedersen et al. (2004).

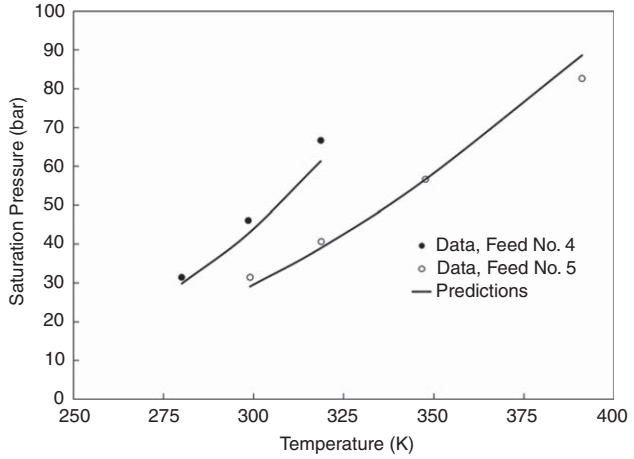

Fig. 7—Saturation pressures measured and predicted for two mixtures with Lloydminster heavy oil, Oil 4 in Table 4—Feeds Nos. 4 and 5 in Li et al. (2013a). The AARD of the saturation-pressure predictions is 6.8% for Feed No. 4 and 4.7% for Feed No. 5.

three-phase region is predicted with the BIPs developed in this research, but not for the zero-BIPs and PR-BIPs cases. The boundary between the two- and single-phase regions is also more accurate with the new BIPs.

The new BIPs may be used with conventional characterization methods instead of the PnA method. Oils Nos. 1 through 5 given in Table 3 were characterized by use of the critical-parameter correlations of Riazi and Daubert (1980) and the acentric-factor correlation of Korsten (2000), along with the compositional characterization described previously as Step 1. However, saturation pressures for the five oils were predicted to be higher than the corresponding experimental data, and the average deviation was 18%. Unlike with the PnA method, it may not be easy to control phase-behavior predictions in a systematic, monotonic manner with conventional methods of fluid characterization, in which various EOS-related parameters are adjusted with little physical justification.

The results presented in this subsection show the importance of the use of the BIPs developed in this research. The PnA method was shown to improve the reliability of reservoir-fluid characterization by the monotonic and systematic change in phase-behavior predictions (Kumar and Okuno 2013, 2015) (Fig. 2). Without the developed BIPs, however, the PR-EOS with the PnA-based

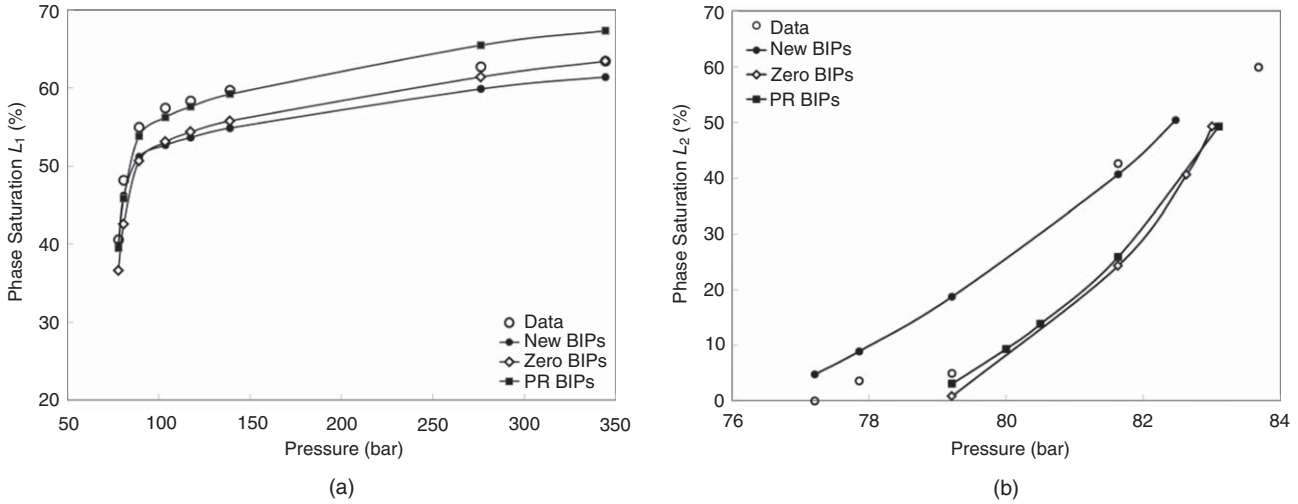

Fig. 8—Liquid-phase saturations for West Sak heavy oil (Oil 1 in Table 4) mixed with CO_2 at 299.81 K. (a) Oleic (L_1) phase; (b) solvent-rich-liquid (L_2) phase.

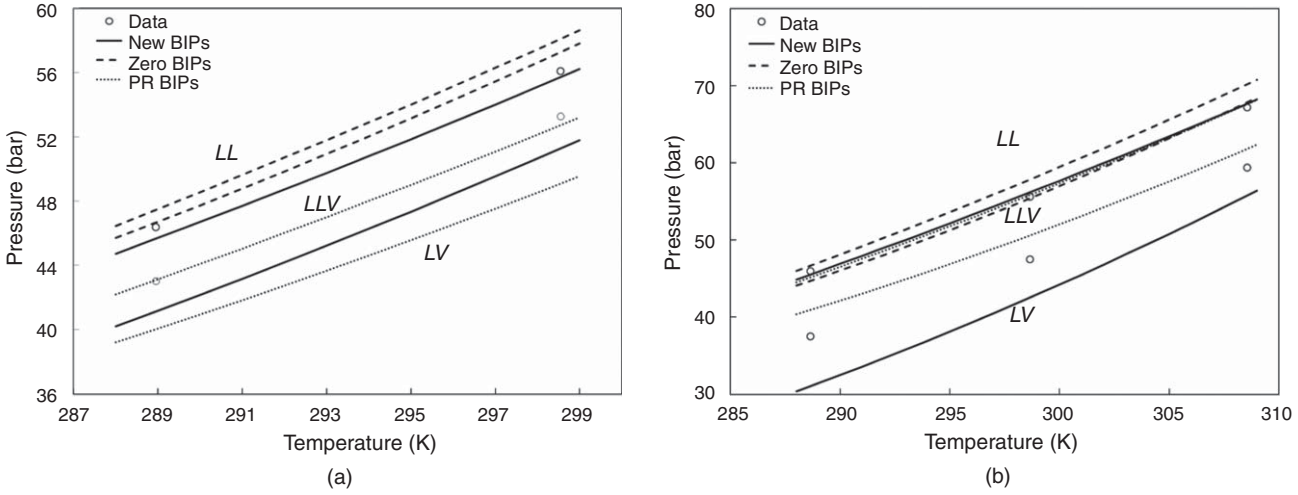

Fig. 9—Three-phase boundaries. (a) Feed No. 14 of Li et al. (2013b), consisting of 23.6% propane, 67.2% CO_2, and 9.2% heavy oil. (b) Feed No. 15 of Li et al. (2013b), consisting of 11.8% butane, 83.2% CO_2, and 5.0% heavy oil. The heavy oil is from Lloydminster (Table 4).

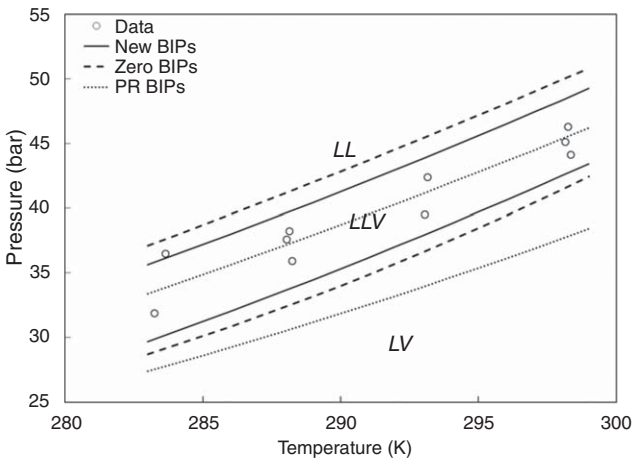

Fig. 10—Three-phase boundaries measured and predicted for a mixture of Athabasca bitumen: 51.0% CO_2, 34.7% propane, and 14.3% bitumen (Badamchi-Zadeh et al. 2009).

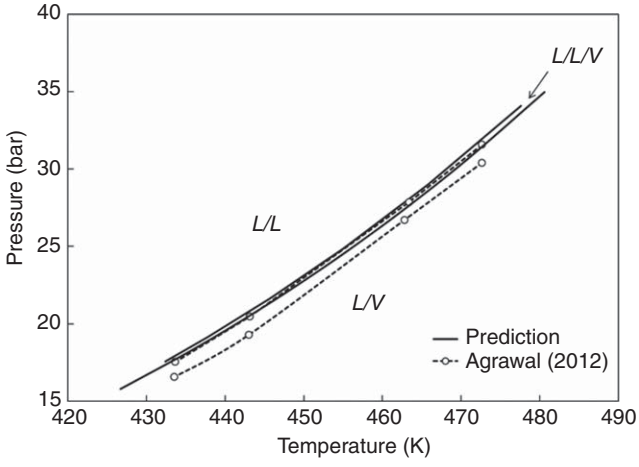

Fig. 11—Three-phase boundaries measured and predicted for a mixture of Peace River bitumen: 89.90% pentane and 10.10% bitumen. The bitumen was characterized by use of the data from Mehrotra and Svrcek (1985). Three-phase boundaries simulated by Agrawal (2012) are also shown.

Oil No.	References	MW (g/mol)	Temperature (K)	β	k	p
1	Turek et al. (1988), Oil B1	149.62	314.26	1.550	4921	6.0
2	Turek et al. (1988), Oil B2	151.22	314.26	1.184	3302	6.1
3	Turek et al. (1988), Oil C2	140.30	313.71	1.454	4477	6.1
4	Turek et al. (1988), Oil D	182.42	313.71	1.551	4577	6.9
5	Khan et al. (1992), Oil BSB	148.88	313.71	1.458	4826	5.6
6	Winzinger et al. (1991), Oil NWE	138.45	301.48	1.325	4037	5.8
7	Khan et al. (1992), Oil JEMA	156.72	316.48	1.113	3092	5.2
8	Shelton and Yarborough (1977), Oil-B	161.47	307.60	1.470	4536	7.5
9	Creek and Sheffield (1993), Oil G	113.13	307.60	1.311	4290	5.8

Table 5—Characterization results for oils for which three phases with CO_2 were reported in the literature. Parameters β and k are defined in the algorithm section. Parameter p indicates the degree of freedom in the chi-squared distribution.

regression scheme may fail to predict three phases or give erroneous multiphase-behavior predictions. The BIPs developed in this research are recommended for use as default BIPs for reliable multiphase-behavior calculations, which can be further adjusted as needed.

The reliability of the new algorithm was further tested by simulating the 1D displacement of West Sak oil by enriched gas in the presence of three hydrocarbon phases (Okuyiga 1992; DeRuiter et al. 1994; Mohanty et al. 1995). In Appendix B, simulation results are compared with experimental data presented by Okuyiga (1992). Results from simulations with the EOS model developed by the new algorithm are consistent with experimental results, in which oil recovery is nonmonotonic with respect to gas enrichment. Although oil-recovery simulations are also affected by other factors, such as relative permeability, viscosity, densities, and dispersion, the level of miscibility in this complex oil displacement is reasonably represented by the EOS model developed.

The analysis of multiphase-behavior predictions in this research has indicated that the simple algorithm is reliable even with the limited PVT data used (P_S and liquid density). However, further adjustment of parameters may be required if additional phase-behavior data are to be matched. Obvious candidates are BIPs for solvents with pseudocomponents. In particular, CO_2 BIPs may be adjusted to accommodate the effects of oil aromaticity and reservoir temperature on compositional phase behavior for CO_2 flooding. Also, the parameters N and β in the algorithm can be flexible; e.g., N can be different for T_C, P_C, and ω.

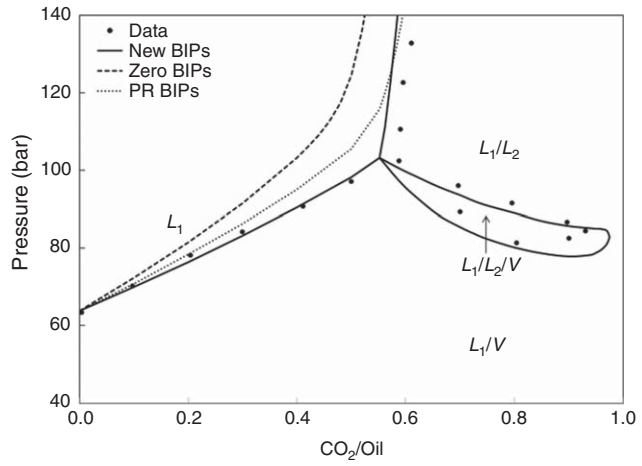

Fig. 12—Comparison of the predicted *P-x* diagram with data for Oil C2 (Table 5) of Turek et al. (1988) with CO_2 at 313.71 K.

Conclusions

A new algorithm was presented for characterization of multiphase behavior for solvent-injection simulation. The PR-EOS was used with the van der Waals mixing rules. The developed algorithm requires only the saturation pressure and liquid density for a given composition and reservoir temperature, in its simplest form. Case studies were conducted for 90 reservoir fluids and their mixtures with solvents for up to three hydrocarbon phases. Conclusions are as follows:

1. The algorithm with the BIPs developed in this research enables the PR-EOS to give reliable predictions of multiphase behavior for reservoir fluids. With the two conventional sets of BIPs tested in this research, the PR-EOS models were less reliable for three-phase predictions for the cases tested in this research.
2. The PnA method was found to be applicable for multiphase characterization; that is, the effect of aromaticity on phase behavior can be modeled through T_C, P_C, and ω of pseudocomponents as monotonic functions of a single parameter in the regression algorithm developed.
3. Results show that positive BIPs are required for the PR-EOS to properly represent three-hydrocarbon-phase behavior of reservoir fluids. The fundamental reason comes from the necessity for accurate predictions of binary three-phase curves. This is in contrast to the use of zero BIPs for hydrocarbon pairs, which has been recommended for simpler two-phase characterization in the literature.

Nomenclature

A = aromatics
k = number of iterations in the algorithm
K = BIPs (Eqs. 8 through 13)
L_1, L_2, V = three hydrocarbon phases, with L_1 #oleic, L_2 #solvent-rich liquid, and V #gaseous
n = number of pseudocomponents
p = degree of freedom in the chi-squared distribution
P_C = critical pressure, bar
P_{CH} = critical pressure calculated from Eq. 6, bar
P_{CP} = critical pressure calculated from Eq. 2, bar
P_S = experimental saturation pressure, bar
P_{S_EOS} = calculates saturation pressure with the PR-EOS and pseudocomponents assumed as n-alkanes, bar
T_C = critical temperature, K
T_{CH} = critical temperature calculated from Eq. 5, K
T_{CP} = critical temperature calculated from Eq. 1, K
β = ratio of experimental and predicted saturation pressures (with PR-EOS, with pseudocomponents as n-alkanes)
δ = deviation of calculated saturation pressure from experimental value
δ_{TOL} = tolerance set for deviation (δ)

ω = acentric factor
ω_H = acentric factor calculated from Eq. 7
ω_P = acentric factor calculated from Eq. 3
$\acute{\omega}_P$ = acentric factor calculated from Eq. 4

Subscript

i = index for pseudocomponent

Acknowledgment

This research was supported by the Natural Sciences and Engineering Research Council of Canada, Japan Petroleum Exploration Company, Limited, and Japan Canada Oil Sands Limited.

References

Aghbash, V. N. and Ahmadi, M. 2012. Evaluation of CO_2-EOR and Sequestration in Alaska West Sak Reservoir Using Four-Phase Simulation Model. Presented at the SPE Western Regional Meeting, Bakersfield, California, 21–23 March. SPE-153920-MS. http://dx.doi.org/10.2118/153920-MS.

Agrawal, P. 2012. *Measurement and Modeling of the Phase Behavior of Solvent Diluted Bitumens*. Master's thesis, University of Calgary.

Akpabio, J. U., Udofia, E. E. and Ogbu, M. 2014. PVT Fluid Characterization and Consistency Check for Retrograde Condensate Reservoir Modeling. Presented at SPE Nigeria Annual International Conference and Exhibition, Lagos, Nigeria, 5–7 August. SPE-172359-MS. http://dx.doi.org/10.2118/172359-MS.

Al-Meshari, A. 2004. *New Strategic Method to Tune Equation of State to Match Experimental Data for Compositional Simulation*. PhD dissertation, Texas A&M University, College Station, Texas.

Al-Subai, K. O. 2001. *Compositional Gradient Calculations for a Saudi Arabian Gas Condensate Reservoir*. Master's thesis, King Fahd University of Petroleum & Minerals, Dhahran, Saudi Arabia.

Badamchi-Zadeh, A., Yarranton, H. W., Svrcek, W. Y. et al. 2009. Phase Behavior and Physical Property Measurements for VAPEX Solvents: Part I. Propane and Athabasca Bitumen. *J Can Pet Technol* **48** (1): 54–61. http://dx.doi.org/10.2118/09-01-54.

Calsep. 2012. PVTsim, Version 19.2.0. Lyngby, Denmark: Calsep.

Chang, H. L., Hurt, L. J. and Kobayashi, R. 1966. Vapour-Liquid Equilibria of Light Hydrocarbons at Low Temperatures and High Pressures: The Methane-*n*-Heptane System. *AIChE J*. **12** (6): 1212–1216. http://dx.doi.org/10.1002/aic.690120629.

Chang, Y.-B. 1990. *Development and Application of an Equation of State Compositional Simulator*. PhD dissertation, University of Texas at Austin, Austin, Texas (August 1990).

Chang, Y.-B., Pope, G. A. and Sepehrnoori, K. 1990. A Higher-Order Finite-Difference Compositional Simulator. *J. Pet. Sci. Eng.* **5** (1): 35–50. http://dx.doi.org/10.1016/0920-4105(90)90004-M.

Choi, E. and Yeo, S. 1998. Critical Properties for Carbon Dioxide + *n*-Alkane Mixtures Using a Variable-Volume View Cell. *J. Chem. Eng. Data* **43** (5): 714–716. http://dx.doi.org/10.1021/je9800297.

Cismondi, M., Nuñez, D. N., Zabaloy, M. S. et al. 2006. GPEC: A Program for Global Phase Equilibrium Calculations in Binary Systems. Oral presentation given at the EQUIFASE VII Iberoamerican Conference on Phase Equilibria and Fluid Properties for Process Design, Morelia, Mexico, 21–25 October.

Coats, K. H. 1985. Simulation of Gas Condensate Reservoir Performance. *J Pet Technol* **37** (10): 1870–1886. SPE-10512-PA. http://dx.doi.org/10.2118/10512-PA.

Coats, K. H. and Smart, G. T. 1986. Application of a Regression-Based EOS PVT Program to Laboratory Data. *SPE Res Eng* **1** (3): 277–299. SPE-11197-PA. http://dx.doi.org/10.2118/11197-PA.

Corey, A. T. 1954. The Interrelation Between Gas and Oil Relative Permeability. *Prod. Monthly*. (November): 38–41.

Creek, J. L. and Sheffield, J. M. 1993. Phase Behavior, Fluid Properties, and Displacement Characteristics of Permian Basin Reservoir Fluid/CO_2 Systems. *SPE Res Eval & Eng* **8** (1): 34–42. SPE-20188-PA. http://dx.doi.org/10.2118/20188-PA.

Danesh, A. 1998. *PVT and Phase Behavior of Petroleum Reservoir Fluids*, first edition. Amsterdam: Elsevier Science B.V.

DeRuiter, R. A., Nash, L. J. and Singletary, M. S. 1994. Solubility and Displacement Behavior of a Viscous Crude with CO_2 and Hydrocarbon Gases. *SPE Res Eng* **9** (2): 101–106. SPE-20523-PA. http://dx.doi.org/10.2118/20523-PA.

Dickson, J. L., Clingman, S., Dittaro, L. M. et al. 2011. Design Approach and Early Field Performance for a Solvent-Assisted SAGD Pilot at Cold Lake, Canada. Presented at the SPE Heavy Oil Conference and Exhibition, Kuwait City, Kuwait, 12–14 December. SPE-150639-MS. http://dx.doi.org/10.2118/150639-MS.

Drohm, J. K., Trengove, R. D. and Goldthrope, W. H. 1988. On the Quality of Data from Standard Gas-Condensate PVT Experiments. Presented at the SPE Gas Technology Symposium, Dallas, 13–15 June. SPE-17768-MS. http://dx.doi.org/10.2118/17768-MS.

Ekundayo, J. M. 2012. *Configuration of Slim Tube Apparatus for Consistent Determination of Minimum Miscibility Pressure (MMP) Data*. Master's thesis, The Petroleum Institute, Abu Dhabi.

Enick, R., Holder, G. D. and Morsi, B. I. 1985. Critical and Three Phase Behavior in the Carbon Dioxide/Tridecane System. *Fluid Phase Equilibr.* **22** (2): 209–224. http://dx.doi.org/10.1016/0378-3812(85)85020-2.

Estrera, S. S. and Luks, K. D. 1987. Liquid-Liquid-Vapor Equilibrium Behavior of Certain Ethane + n-Paraffin Mix. *J. Chem. Eng. Data*. **32** (2): 201–204. http://dx.doi.org/10.1021/je00048a022.

Fall, D. J. and Luks, K. D. 1985. Liquid-Liquid-Vapor Phase Equilibria of the Binary System Carbon Dioxide + n-Tridecane. *J. Chem. Eng. Data* **30** (3): 276–279. http://dx.doi.org/10.1021/je00041a012

Fall, D. J., Fall, J. L. and Luks, K. D. 1985. Liquid-Liquid-Vapor Immiscibility Limits in Carbon Dioxide + n-Paraffin Mixtures. *J. Chem. Eng. Data* **30** (1): 82–88. http://dx.doi.org/10.1021/je00039a028.

Fawumi, O. K. 1999. *Effect of Liquid Drop-out on the Productivity of a Rich Gas Condensate Reservoir*. Master's thesis, King Fahd University of Petroleum & Minerals, Dhahran, Saudi Arabia.

Firoozabadi, A. and Khalid, A. 1986. Analysis and Correlation of Nitrogen and Lean-Gas Miscibility Pressure. *SPE Res Eng* **1** (6): 575–582. SPE-13669-PA. http://dx.doi.org/10.2118/13669-PA.

Firoozabadi, A., Hekim, Y. and Katz, D. L. 1978. Reservoir Depletion Calculations for Gas Condensates Using Extended Analyses in the Peng-Robinson Equation of State. *Can. J. Chem. Eng.* **56** (5): 610–615. http://dx.doi.org/10.1002/cjce.5450560515.

Fulco, G. J. 1999. Case History of Miscible Gas Flooding in the Powder River Basin North Buck Draw Unit. Presented at the SPE Rocky Mountain Regional Meeting, Gillette, Wyoming, 15–18 April. SPE-55634-MS. http://dx.doi.org/10.2118/55634-MS.

Gajda, M. 2014. *Comparison of Black Oil Tables and EOS Fluid Characterization in Reservoir Simulation*. Master's thesis. University of Miskolc, Miskolc, Hungary.

Gao, W., Robinson, R. L. Jr. and Gasem, K. A. M. 2001. Improved Correlations for Heavy *n*-Paraffin Physical Properties. *Fluid Phase Equilibr.* **179** (1–2): 207–216. http://dx.doi.org/10.1016/S0378-3812(00)00498-2.

Godbole, S. P., Thele, K. J. and Reinbold, E. W. 1995. EOS Modeling and Experimental Observations of Three-Hydrocarbon-Phase Equilibria. *SPE Res Eng* **10** (2): 101–108. SPE-24936-PA. http://dx.doi.org/10.2118/24936-PA.

Graue, D. J. and Zana, E. T. 1981. Study of a Possible CO_2 Flood in Rangely Field. *J Pet Technol* **33** (7): 1312–1318. SPE-7060-PA. http://dx.doi.org/10.2118/7060-PA.

Gregorowicz, J., De Loos, T. W. and De Swaan Arons, J. 1993a. Liquid-Liquid-Vapour Phase Equilibria in the System Ethane + Propane + Eicosane: Retrograde Behaviour of the Heavy Liquid Phase. *Fluid Phase Equilibr.* **84** (1 April): 225–250. http://dx.doi.org/10.1016/0378-3812(93)85125-6.

Gregorowicz, J., Smits, P. J., de Loos, T. W. et al. 1993b. Liquid-Liquid-Vapour Phase Equilibria in the System Methane + Ethane + Eicosane: Retrograde Behaviour of the Heavy Liquid Phase. *Fluid Phase Equilibr.* **85** (15 May): 225–238. http://dx.doi.org/10.1016/0378-3812(93)80016-G.

Guler, B., Wang, P., Delshad, M. et al. 2001. Three- and Four- Phase Flow Compositional Simulations of CO_2/NGL EOR. Presented at the SPE Annual Technical Conference and Exhibition, New Orleans, 30 September–3 October. SPE-71485-MS. http://dx.doi.org/10.2118/71485-MS.

Guo, T. M. and Du, L. 1989. A New Three-Parameter Cubic Equation of State for Reservoir Fluids. III. Application to Gas Condensates. SPE 19374-MS, unsolicited.

Gupta, S. C. and Gittins, S. D. 2006. Christina Lake Solvent Aided Process Pilot. *J Can Pet Technol* **45** (9): 15–18. PETSOC-06-09-TN. http://dx.doi.org/10.2118/06-09-TN.

Gupta, S. C., Gittins, S. and Picherack, P. 2005. Field Implementation of Solvent Aided Process. *J Can Pet Technol* **44** (11): 8–13. PETSOC-05-11-TN1. http://dx.doi.org/10.2118/05-11-TN1.

Heidemann, R. A. and Khalil, A. M. 1980. The Calculation of Critical Points. *AIChE J*. **26** (5): 769–779. http://dx.doi.org/10.1002/aic.690260510.

Henry, R. L. and Metcalfe, R. S. 1983. Multiple-Phase Generation During Carbon Dioxide Flooding. *SPE J*. **23** (4): 595–601. SPE-8812-PA. http://dx.doi.org/10.2118/8812-PA.

Høier, L. 1997. *Miscibility Variation in Compositional Grading*. PhD dissertation, Norwegian University of Science and Technology, Trondheim, Norway.

Horn, L. D. V. and Kobayashi, R. 1967. Vapor-Liquid Equilibria of Light Hydrocarbons at Low Temperatures and Elevated Pressures in Hydrocarbon Solvents. Methane-Propane-*n*-Heptane, Methane-Ethane-*n*-Heptane, and Methane-Propane-Toluene Systems. *J. Chem. Eng. Data* **12** (3): 294–303. http://dx.doi.org/10.1021/je60034a004.

Hosein, R., Jagai, T. and Dawe, R. A. 2013. A Method for Predicting the Phase Behaviour of Trinidad Gas Condensates. *W. Indian J. Eng.* **35** (2): 22–30.

Hottovy, J. D., Luks, K. D. and Kohn, J. P. 1981a. Three-Phase Liquid-Liquid-Vapor Equilibriums Behavior of Certain Binary Carbon Dioxide-*n*-Paraffin Systems. *J. Chem. Eng. Data* **26** (3): 256–258. http://dx.doi.org/10.1021/je00025a009.

Hottovy, J. D., Kohn, J. P. and Luks, K. D. 1981b. Partial Miscibility Behavior of the Methane-Ethane-*n*-Octane System. *J. Chem. Eng. Data* **26** (2): 135–137. http://dx.doi.org/10.1021/je00024a009.

Hottovy, J. D., Kohn, J. P. and Luks, K. D. 1982. Partial Miscibility Behavior of the Ternary Systems Methane-Propane-*n*-Octane, Methane-*n*-Butane-*n*-Octane, and Methane-Carbon Dioxide-*n*-Octane. *J. Chem. Eng. Data* **27** (3): 298–302. http://dx.doi.org/10.1021/je00029a020.

Jacoby, R. H. and Yarborough, L. 1967. PVT Measurements on Petroleum Reservoir Fluids and Their Uses. *Ind. Eng. Chem.* **59** (10): 48–62. http://dx.doi.org/10.1021/ie50694a010.

Jacoby, R. H., Koeller, R. C. and Berry, V. J. Jr. 1959. Effect of Composition and Temperature on Phase Behavior and Depletion Performance of Rich Gas-Condensate Systems. *J Pet Technol* **11** (7): 58–63. SPE-1093-G. http://dx.doi.org/10.2118/1093-G.

Jangkamolkulchai, A. and Luks, K. D. 1989. Partial Miscibility Behavior of the Methane + Ethane + *n*-Docosane and the Methane + Ethane + *n*-Tetradecylbenzene Ternary Mixtures. *J. Chem. Eng. Data* **34** (1): 92–99. http://dx.doi.org/10.1021/je00055a027.

Jaubert, J-N., Avaullee, L. and Souvay, J-F. 2002. A Crude Oil Data Bank Containing More Than 5000 PVT and Gas Injection Data. *J. Pet. Sci. Eng.* **34** (1–4): 65–107. http://dx.doi.org/10.1016/S0920-4105(02)00153-5.

Kato, K., Nagahama, K. and Hirata, M. 1981. Generalized Interaction Parameters for the Peng-Robinson Equation of State: Carbon Dioxide—*n*-Paraffin Binary Systems, *Fluid Phase Equilibr*. **7** (3–4): 219–231. http://dx.doi.org/10.1016/0378-3812(81)80009-X.

Kenyon, D. E. and Behie, G. A. 1987. Third SPE Comparative Solution Project: Gas Cycling of Retrograde Condensate Reservoirs. *J Pet Technol* **39** (8): 981–997. SPE-12278-PA. http://dx.doi.org/10.2118/12278-PA.

Khan, S. A., Pope, G. A. and Sepehrnoori, K. 1992. Fluid Characterization of Three-Phase CO_2/Oil Mixtures. Presented at the SPE/DOE Enhanced Oil Recovery Symposium, Tulsa, 22–24 April. SPE-24130-MS. http://dx.doi.org/10.2118/24130-MS.

Kilgren, K. H. 1966. Phase Behavior of a High-Pressure Condensate Reservoir Fluid. *J Pet Technol* **18** (8): 1001–1005. SPE-1277-PA. http://dx.doi.org/10.2118/1277-PA.

Koch, H. A. Jr. and Hutchinson, C. A. Jr. 1958. Miscible Displacements of Reservoir Oil Using Flue Gas. In *Petroleum Transactions, AIME*, Vol. 213, 7–10. SPE-912-G.

Kordas, A., Tsoutsouras, K., Stamataki, S. et al. 1994. A Generalized Correlation for the Interaction Coefficients of CO_2—Hydrocarbon Binary Mixtures. *Fluid Phase Equilibr*. **93** (11 February): 141–166. http://dx.doi.org/10.1016/0378-3812(94)87006-3.

Korsten, H. 2000. Internally Consistent Prediction of Vapor Pressure and Related Properties. *Ind. Eng. Chem. Res.* **39** (3): 813–820. http://dx.doi.org/10.1021/ie990579d.

Krejbjerg, K. and Pedersen, K. S. 2006. Controlling VLLE Equilibrium with a Cubic EoS in Heavy Oil Modeling. Presented at Canadian International Petroleum Conference, Calgary, 13–15 June. PETSOC-2006-052. http://dx.doi.org/10.2118/2006-052.

Kukarni, A. A., Zarah, B. Y., Luks, K. D. et al. 1974. Phase-Equilibriums Behavior of System Carbon Dioxide-*n*-Decane at Low Temperatures. *J. Chem. Eng. Data* **19** (1): 92–94. http://dx.doi.org/10.1021/je60060a005.

Kumar, A. and Okuno, R. 2012. Critical Parameters Optimized for Accurate Phase Behavior Modeling for Heavy n-Alkanes up to C_{100} using the Peng–Robinson Equation of State. *Fluid Phase Equilibr*. **335** (15 December): 46–59. http://dx.doi.org/10.1016/j.fluid.2012.07.029.

Kumar, A. and Okuno, R. 2013. Characterization of Reservoir Fluids Using an EOS based on Perturbation from *n*-Alkanes. *Fluid Phase Equilibr*. **358** (25 November): 250–271. http://dx.doi.org/10.1016/j.fluid.2013.08.035.

Kumar, A. and Okuno, R. 2015. Direct Perturbation of the Peng–Robinson Attraction and Covolume Parameters for Reservoir Fluid Characterization. *Chem. Eng. Sci.* **127** (4 May): 293–309. http://dx.doi.org/10.1016/j.ces.2015.01.032.

Lee, J. I. and Reitzel, G. A. 1982. High Pressure, Dry Gas Miscible Flood Brazeau River Nisku Oil Pools. *J Pet Technol* **34** (11): 2503–2509. SPE-10243-PA. http://dx.doi.org/10.2118/10243-PA.

Li, H., Zheng, S. and Yang. D. 2013a. Enhanced Swelling Effect and Viscosity Reduction of Solvent(s)/CO_2/Heavy-Oil Systems. *SPE J.* **18** (4): 695–707. SPE-150168-PA. http://dx.doi.org/10.2118/150168-PA.

Li, X., Li, H. and Yang, D. 2013b. Determination of Multiphase Boundaries and Swelling Factors of Solvent(s)-CO_2-Heavy Oil Systems at High Pressures and Elevated Temperatures. *Energ. Fuel.* **27** (3): 1293–1306. http://dx.doi.org/10.1021/ef301866e.

Lin, H. 1984. Peng-Robinson Equation of State for Vapor-Liquid Equilibrium Calculations for Carbon dioxide + Hydrocarbon Mixtures. *Fluid Phase Equilibr*. **16** (2): 151–169. http://dx.doi.org/10.1016/0378-3812(84)85028-1.

Lin, Y.-N., Chen, R. J. J., Chappelear, P. S. et al. 1977. Vapor-Liquid Equilibrium of the Methane-n-Hexane System at Low Temperature. *J. Chem. Eng. Data* **22** (4): 402–408. http://dx.doi.org/10.1021/je60075a007.

Llave, F. M., Luks, K. D. and Kohn, J. P. 1987. Three-Phase Liquid-Liquid-Vapor Equilibria in the Nitrogen-Methane-Ethane and Nitrogen-Methane-Propane Systems. *J. Chem. Eng. Data* **32** (1): 14–17. http://dx.doi.org/10.1021/je00047a004

Lohrenz, J., Bray, B. G. and Clark, C. R. 1964. Calculating Viscosities of Reservoir Fluids from Their Compositions. *J Pet Technol* **16** (10): 1171–1176. SPE-915-PA. http://dx.doi.org/10.2118/915-PA.

Malik, Q. M. and Islam, M. R. 2000. CO_2 Injection in the Weyburn Field of Canada: Optimization of Enhanced Oil Recovery and Greenhouse Gas Storage with Horizontal Wells. Presented at the SPE/DOE Improved Oil Recovery Symposium, Tulsa, 3–5 April. SPE-59327-MS. http://dx.doi.org/10.2118/59327-MS.

McGuire, P. L., Spence, A. P. and Redman, R. S. 2001. Performance Evaluation of a Mature Miscible Gasflood at Prudhoe Bay. *SPE Res Eval & Eng* **4** (4): 318–326. SPE-72466-PA. http://dx.doi.org/10.2118/72466-PA.

McVay, D. A. 1994. *Generalization of PVT Properties for Modified Black-Oil Simulation of Volatile and Gas Condensate Reservoirs*. PhD dissertation, Texas A&M University, College Station, Texas.

Mehrotra, A. K. and Svrcek, W. Y. 1985. Viscosity, Density and Gas Solubility Data for Oil Sand Bitumens; Part II, Peace River Bitumen Saturated with N_2, CO, CH_4, CO_2, and C_2H_6. *AOSTRA J. Res.* **1** (4): 269–279.

Metcalfe, R. S. and Raby, W. J. 1986. Phase Equilibria for a Rich Gas Condensate-Nitrogen System. *Fluid Phase Equilibr*. **29** (October): 563–573. http://dx.doi.org/10.1016/0378-3812(86)85055-5.

Mizenko, G. J. 1992. North Cross (Devonian) Unit CO_2 Flood: Status Report. Presented at the SPE/DOE Enhanced Oil Recovery

Symposium, Tulsa, 22–24 April. SPE-24210-MS. http://dx.doi.org/10.2118/24210-MS.

Mohanty, K. K., Masino, W. H. Jr., Ma, T. D. et al. 1995. Role of Three-Hydrocarbon-Phase Flow in a Gas-Displacement Process. *SPE Res Eng* **10** (3): 214–221. SPE-24115-PA. http://dx.doi.org/10.2118/24115-PA.

Moore, D. C. 1989. *Simulation of Gas-Condensate Reservoir Performance Using Schmidt-Wenzel Equation of State*. Master's thesis, Montana College of Mineral Science and Technology, Butte, Montana.

Mushrif, S. H. 2004. *Determining Equation of State Binary Interaction Parameters Using K- and L-Points*. Master's thesis, University of Saskatchewan, Saskatoon, Canada (October 2004).

Negahban, S. and Kremesec, V. J. Jr. 1989. Development and Validation of Equation-of-State Fluid Descriptions for CO_2-Reservoir Oil Systems. Presented at the 64th Annual Technical Conference and Exhibition, San Antonio, Texas, 8–11 March. SPE 19637-PA. http://dx.doi.org/10.2118/19637-PA.

Negahban, S., Pedersen, K. S., Baisoni, M. A. et al. 2010. An EoS Model for a Middle East Reservoir Fluid with an Extensive EOR PVT Data Material, Presented at Abu Dhabi International Petroleum Exhibition and Conference, Abu Dhabi, 1–4 November. SPE-136530-MS. http://dx.doi.org/10.2118/136530-MS.

Nghiem, L. X. and Li, Y. K. 1986. Effect of Phase Behavior on CO_2 Displacement Efficiency at Low Temperatures: Model Studies With an Equation of State. *SPE Res Eng* **1** (4): 414–422. SPE-13116-PA. http://dx.doi.org/10.2118/13116-PA.

Nikitin, E. D. and Popov, A. P. 2015. Critical Point Measurement of Some Polycyclic Aromatic Hydrocarbons. *J. Chem. Thermodyn.* **80** (January): 124–127. http://dx.doi.org/10.1016/j.jct.2014.09.004.

Okuno, R. and Xu, Z. 2014a. Mass Transfer on Multiphase Transitions in Low-Temperature Carbon-Dioxide Floods. *SPE J.* **19** (6): 1005–1023. SPE-166345-PA. http://dx.doi.org/10.2118/166345-PA.

Okuno, R. and Xu, Z. 2014b. Efficient Displacement of Heavy Oil by Use of Three Hydrocarbon Phases. *SPE J.* **19** (5): 956–973. SPE-165470-PA. http://dx.doi.org/10.2118/165470-PA.

Okuyiga, M. O. 1992. Equation of State Characterization and Miscibility Development in a Multiple Phase Hydrocarbon System. Presented at the SPE Annual Technical Conference and Exhibition, Washington, DC, 4–7 October. SPE-24937-MS. http://dx.doi.org/10.2118/24937-MS.

Pedersen, K. S. and Christensen, P. L. 2007. *Phase Behavior of Petroleum Reservoir Fluids*. Boca Raton, Florida: CRC Press.

Pedersen, K. S., Milter, J. and Sørensen, H. 2004. Cubic Equations of State Applied to HT/HP and Highly Aromatic Fluids. *SPE J.* **9** (2): 186–192. SPE-88364-PA. http://dx.doi.org/10.2118/88364-PA.

Pedersen, K. S., Thomassen, P. and Fredenslund, A. 1989. Characterization of Gas Condensate Mixtures. In *Advances in Thermodynamics*, ed. L. G. Chorn and G. A. Mansoori, 137–152. New York City: Taylor & Francis.

Peng, D.-Y. and Robinson, D. B. 1976. A New Two-Constant Equation of State. *Ind. Eng. Chem. Fund.* **15** (1): 59–64. http://dx.doi.org/10.1021/i160057a011.

Peng, D.-Y. and Robinson, D. B. 1978. The Characterization of the Heptanes and Heavier Fractions for the GPA Peng-Robinson Programs. Research Report No. RR-28, Gas Processors Association, Tulsa.

Peters, C. J. 1994. Multiphase Equilibria in Near-Critical Solvents. In *Supercritical Fluids*, ed. E. Kiran and J. M. H. Levelt Sengers, 117–145. Dordrecht, The Netherlands: Springer.

Peters, C. J., de Roo, J. L. and De Swaan Arons, J. 1992. Measurements and Calculations of Phase Equilibria in Binary Mixtures of Propane + Tetratriacontane. *Fluid Phase Equilibr.* **72** (March): 251–266. http://dx.doi.org/10.1016/0378-3812(92)85029-8.

Peters, C. J., de Roo, J. L. and De Swaan Arons, J. 1993. Phase Equilibria in Binary Mixtures of Propane and Hexacontane. *Fluid Phase Equilibr.* **85** (15 May): 301–312. http://dx.doi.org/10.1016/0378-3812(93)80021-E.

Peters, C. J., Lichtenthaler, R. N. and De Swaan Arons, J. 1986. Three Phase Equilibria in Binary Mixtures of Ethane and Higher *n*-Alkanes. *Fluid Phase Equilibr.* **29** (October): 495–504. http://dx.doi.org/10.1016/0378-3812(86)85048-8.

Peters, C. J., Van der Kooi, H. J. and De Swaan Arons, J. 1987a. Measurements and Calculations of Phase Equilibria for (Ethane + Tetracosane) and (p, $V_{m'}^*$, T) of Liquid Tetracosane. *J. Chem. Thermodyn.* **19** (4): 395–405. http://dx.doi.org/10.1016/0021-9614(87)90125-X.

Peters, C. J., de Roo, J. L. and De Swaan Arons, J. 1987b. Three-Phase Equilibria in (Ethane + Pentacosane). *J. Chem. Thermodyn.* **19** (3): 265–272. http://dx.doi.org/10.1016/0021-9614(87)90134-0.

Peters, C. J., Van Der Kooi, H. J., De Roo, J. L. et al. 1989. The Search for Tricriticality in Binary Mixtures of Near-Critical Propane and Normal Paraffins. *Fluid Phase Equilibr.* **51** (November): 339–351. http://dx.doi.org/10.1016/0378-3812(89)80375-9.

Quiñones-Cisneros, S. E., Zéberg-Mikkelsen, C. K., Baylaucq, A. et al. 2004. Viscosity Modeling and Prediction of Reservoir Fluids: From Natural Gas to Heavy Oils. *Int. J. Therm.* **25** (5): 1353–1366. http://dx.doi.org/10.1007/s10765-004-5743-z.

Reamer, H. H. and Sage, B. H. 1963. Phase Equilibria in Hydrocarbon Systems. Volumetric and Phase Behavior of the *n*-Decane-CO_2 System. *J. Chem. Eng. Data* **8** (4): 508–513. http://dx.doi.org/10.1021/je60019a010.

Reid, T. 1994. Study of Hydrocarbon Miscible Solvent Slug Injection Process for Improved Recovery of Heavy Oil From Schrader Bluff Pool, Milne Point Unit, Alaska. Annual Report for DE-FG22-93BC14864 for the US Department of Energy, University of Alaska Fairbanks, Fairbanks, Alaska.

Renner, T. A., Metcalfe, R. S., Yellig, W. F. Jr. et al. 1989. Displacement of Rich Gas Condensate by Nitrogen: Laboratory Corefloods and Numerical Simulations. *SPE Res Eng* **4** (1): 52–58. SPE-16714-PA. http://dx.doi.org/10.2118/16714-PA.

Reudelhuber, F. O. and Hinds, R. F. 1957. A Compositional Material Balance Method for Prediction of Recovery from Volatile Oil Depletion Drive Reservoirs. In *Petroleum Transactions, AIME*, Vol. 210, 19–26. SPE-690-G.

Riazi, M. R. and Daubert, T. E. 1980. Simplify Property Predictions. *Hydrocarb. Process* **59** (3): 115–116.

Rodrigues, A. B. and Kohn, J. P. 1967. Three Phase Equilibria in the Binary Systems Ethane-*n*-Docosane and Ethane-*n*-Octacosane. *J. Chem. Eng. Data* **12** (2): 191–193. http://dx.doi.org/10.1021/je60033a008.

Roper, M. 1989. *An Experimental Study of CO_2/West-Sak-Crude-Oil Phase Behavior*. Master's thesis, University of Alaska Fairbanks, Fairbanks, Alaska.

Secuianu, C., Feroiu, V. and Geana, D. 2007. Investigation of Phase Equilibria in the Ternary System Carbon Dioxide + 1-Heptanol + *n*-Pentadecane. *Fluid Phase Equilibr.* **261** (1–2): 337–342. http://dx.doi.org/10.1016/j.fluid.2007.07.001.

Sharma, A. K., Patil, S. L., Kamath, V.A. et al. 1989. Miscible Displacement of Heavy West Sak Crude by Solvents in Slim Tube. Presented at the SPE California Regional Meeting, Bakersfield, California, 5–7 April. SPE-18761-MS. http://dx.doi.org/10.2118/18761-MS.

Sharma, G. D. 1990. Development of Effective Gas Solvents Including Carbon Dioxide for the Improved Recovery of West Sak Oil. Report No. DOE/FE/61114-2 by the University of Alaska Fairbanks, Fairbanks, Alaska, for the National Petroleum Technology Office, US Department of Energy, Tulsa.

Shelton, J. L. and Yarborough, L. 1977. Multiple Phase Behavior in Porous Media During CO_2 or Rich-Gas Flooding. *J Pet Technol* **29** (9): 1171–1178. SPE-5827-PA. http://dx.doi.org/10.2118/5827-PA.

Soave, G. 1972. Equilibrium Constants from a Modified Redlich-Kwong Equation of State. *Chem. Eng. Sci.* **27** (6): 1197–1203. http://dx.doi.org/10.1016/0009-2509(72)80096-4.

Spivak, A. 1971. *Mathematical Simulation of Condensate-Gas Reservoirs*. PhD dissertation, University of Texas at Austin, Austin, Texas.

Stein, M. H., Frey, D. D., Walker, R. D. et al. 1992. Slaughter Estate Unit CO_2 Flood: Comparison Between Pilot and Field-Scale Performance. *J Pet Technol* **44** (9): 1026–1032. SPE-19375-PA. http://dx.doi.org/10.2118/19375-PA.

Subero, C. L. 2009. *Numerical Modeling of Nitrogen Injection into Gas Condensate Reservoir*. Master's thesis, West Virginia University, Morgantown, West Virginia.

Tanner, C. S., Baxley, P. T., Crump, J. G. III. et al. 1992. Production Performance of the Wasson Denver Unit CO_2 Flood. Presented at the SPE/DOE Enhanced Oil Recovery Symposium, Tulsa, 22–24 April. SPE-24156-MS. http://dx.doi.org/10.2118/24156-MS.

Turek, E. A., Metcalfe, R. S. and Fishback, R. E. 1988. Phase Behavior of Several CO_2/ West Texas-Reservoir-Oil Systems. *SPE Res Eng* **3** (2): 505–516. SPE-13117-PA. http://dx.doi.org/10.2118/13117-PA.

Uzunov, D. I. 1993. *Introduction to the Theory of Critical Phenomena*. Singapore: World Scientific Publishing.

Van der Steen, J., De Loos, T. W. and de Swaan, A. J. 1989. The Volumetric Analysis and Prediction of Liquid-Liquid-Vapor Equilibria in Certain Carbon Dioxide + *n*-Alkane Systems. *Fluid Phase Equilibr.* **51** (November): 353–367. http://dx.doi.org/10.1016/0378-3812(89)80376-0.

Varotsis, N., Stewart, G., Todd, A. C. et al. 1986. Phase Behavior of Systems Comprising North Sea Reservoir Fluids and Injection Gases. *J Pet Technol* **38** (11): 1221–1233. SPE-12647-PA. http://dx.doi.org/10.2118/12647-PA.

Vogel, J. L. and Yarborough, L. 1980. The Effect of Nitrogen on the Phase Behavior and Physical Properties of Reservoir Fluids. Presented at SPE/DOE Symposium on Enhanced Oil Recovery, Tulsa, 20–23 April. SPE-8815-MS. http://dx.doi.org/10.2118/8815-MS.

Whitaker, C. A. and Kim, J. S. 1993. Application of Extended Equation of State Work to Optimize the Pegasus Devonian Field Unit No. 3 Gas Cycling Operation. Presented at SPE Annual Technical Conference and Exhibition, Houston, 3–6 October. SPE-26656-MS. http://dx.doi.org/10.2118/26656-MS.

Whitson, C. H. and Torp, S. B. 1983. Evaluating Constant-Volume Depletion Data. *J Pet Technol* **35** (3): 610–620. SPE-10067-PA. http://dx.doi.org/10.2118/10067-PA.

Whitson, C. H. and Belery, P. 1994. Compositional Gradients in Petroleum Reservoirs. Presented at University of Tulsa Centennial Petroleum Engineering Symposium, Tulsa, 29–31 August. SPE-28000-MS. http://dx.doi.org/10.2118/28000-MS.

Whitson, C. H. and Brule, M. R. 2000. *Phase Behavior*, Vol. 20. Richardson, Texas: Monorgraph Series, Society of Petroleum Engineers.

Winzinger, R., Brink, J. L., Patel, K. S. et al. 1991. Design of a Major CO2 Flood, North Ward Estes Field, Ward County, Texas. *SPE Res Eng* **6** (1): 11–16. SPE-19654-PA. http://dx.doi.org/10.2118/19654-PA.

Yaws, C. L. 2010. *Thermo Physical Properties of Chemicals and Hydrocarbons*. New York City: Knovel.

Appendix A—Development of BIPs

BIPs were optimized for CO_2, methane, ethane, and propane with heptane and heavier *n*-alkanes by use of three-phase data, including critical endpoints (CEPs). A CEP is where two phases merge in the presence of the other immiscible phase (Uzunov 1993). For a three-phase region bounded by two CEPs, two liquid phases are critical in the presence of V phase ($L_1 = L_2$–V) at the lower CEP (LCEP). At the upper CEP (UCEP), the V and L_2 phases are critical in the presence of the L_1 phase (L_1–$L_2 = V$). The optimization was concerned primarily with UCEP predictions in this research.

Experimental data are available for UCEPs for the methane binaries with hexane (Lin et al. 1977) and heptane (Chang et al. 1966), for the ethane binaries with *n*-C_{18}, *n*-C_{19}, *n*-C_{20}, *n*-C_{22}, *n*-C_{23}, and *n*-C_{24} (Peters et al. 1986, 1987a; Estrera and Luks 1987), and for the propane binaries with *n*-C_{32}, *n*-C_{34}, *n*-C_{36}, *n*-C_{38}, *n*-C_{40}, *n*-C_{44}, *n*-C_{46}, *n*-C_{50}, and *n*-C_{60} (Peters et al. 1989, 1992, 1993). These data were matched with the PR-EOS by use of an in-house FORTRAN code modeled after the algorithms of Heidemann and Khalil (1980) and Mushrif (2004). The code was validated with the GPEC (Version 3.2.0) software of Cismondi et al. (2006). Critical parameters and ω for CO_2, methane, ethane, and propane were taken from Yaws (2010). The critical parameters of *n*-alkanes heavier than hexane were from Eqs. 1 and 2 of Gao et al. (2001).

In the optimization, the BIP was the only adjustable parameter to match the UCEP for a given binary system. With the PR-EOS with the van der Waals mixing rules, immiscible three-phase points in pressure and temperature were predicted well once the UCEP was matched. However, it was found that matching the LCEP data tends to require a smaller BIP value than matching the UCEP data for a given binary system **(Table A-1).** This may be partly because critical parameters for heavy *n*-alkanes are uncertain and dependent on a correlation (Gao et al. 2001), and partly because of the inherent limitation of the PR-EOS with the van der Waals mixing rules. These two factors affect the PR

				Optimized BIPs	
Components	T_C (K)	P_C (bar)	ω	UCEP	LCEP
CO_2	304.20	73.760	0.2250	–	–
CH_4	190.60	46.000	0.0080	–	–
C_2H_6	305.40	48.840	0.0980	–	–
C_3H_8	369.80	42.460	0.1520	–	–
C_7H_{16}	540.40	27.497	0.3029	0.0497	–
$C_{18}H_{38}$	745.48	12.271	0.7057	0.0424	0.0424
$C_{19}H_{40}$	756.56	11.549	0.7480	0.0419	0.0419
$C_{20}H_{42}$	766.91	10.884	0.7904	0.0403	0.0410
$C_{22}H_{46}$	785.71	9.704	0.8750	0.0400	0.0400
$C_{23}H_{48}$	794.27	9.178	0.9170	0.0435	0.0390
$C_{24}H_{50}$	802.33	8.690	0.9587	0.0437	–
$C_{32}H_{66}$	852.77	5.788	1.2771	0.0553	0.0409
$C_{34}H_{70}$	862.41	5.266	1.3516	0.0572	0.0378
$C_{36}H_{74}$	871.14	4.803	1.4240	0.0597	0.0358
$C_{38}H_{78}$	879.08	4.390	1.4942	0.0631	0.0331
$C_{40}H_{82}$	886.32	4.021	1.5623	0.0657	0.0305
$C_{44}H_{90}$	899.00	3.391	1.6921	0.0681	0.0247
$C_{46}H_{94}$	904.56	3.123	1.7539	0.0645	0.0218
$C_{50}H_{102}$	914.37	2.659	1.8719	0.0696	–
$C_{60}H_{122}$	933.03	1.820	2.1362	0.0455	–

Table A-1—T_C, P_C, and ω used for BIP optimization in terms of UCEP, LCEP, and optimized BIPs.

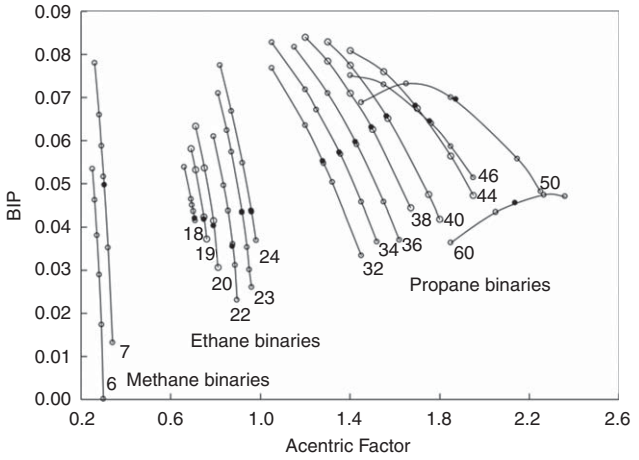

Fig. A-1—Trend of BIP with respect to ω for the heavier *n*-alkane for matching the UCEP data for each binary. The number below a curve indicates the CN of the heavier *n*-alkane. The filled circles are the points used in developing the methane, ethane, and propane BIP correlations (Eqs. 9, 10, and 11). The ω for the filled circles are dependent on Eq. 4.

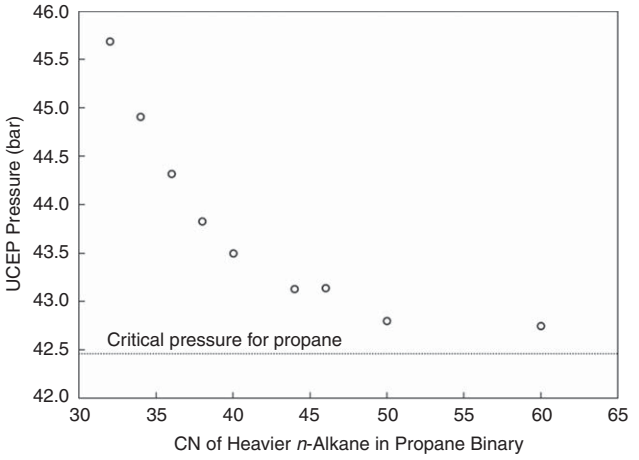

Fig. A-2—UCEP pressures measured for propane binaries (Peters et al. 1989, 1993). The horizontal line shows the critical pressure of propane. Fluctuation in measured UCEP pressure is observed as the critical point of propane is approached.

attraction parameters, to which multiphase-behavior predictions are sensitive. More-accurate representation of three phases bounded by the UCEP and LCEP for a given binary system may require a different form for temperature dependence of the attraction parameter and/or more-sophisticated mixing rules.

It was observed that matching UCEPs with the PR-EOS requires minor deviations from the ω correlation of Gao et al. (2001). To find a smooth ω trend with respect to CN that can be used for matching UCEPs, different pairs of ω and BIP were found for each binary, as shown in **Fig. A-1.** In Fig. A-1, the number below a curve indicates the CN of the heavier *n*-alkane. The curves follow the same trend except for the propane binaries with n-C_{46} and n-C_{60}. The irregularity for these binaries appears to be caused by the fluctuation in the UCEP data measured near the asymptotic limit defined by the critical point of propane, as shown in **Fig. A-2.** This type of irregularity was also observed in terms of measured UCEP temperature, although not shown here.

Eq. 4 gives a smooth trend for nonphysical acentric factor ($\acute{\omega}$) with respect to CN in this research. Although Eq. 4 was found by use of both nonphysical and physical values of ω, the nonphysical values were chosen to be as close to the corresponding physical value as possible. The ω shown by the filled circles in Fig. A-1 have been calculated from Eq. 4. For n-C_{32}, n-C_{34}, n-C_{36}, n-C_{38}, and n-C_{40}, these are nearly equal to their respective physical values as given in Eq. 3 (the AAD is less than 0.015). **Fig. 1** shows the comparison between Eqs. 3 and 4.

The trend of optimized BIPs for the ethane binaries with n-C_{18}, n-C_{19}, n-C_{20}, n-C_{22}, n-C_{23}, and n-C_{24} is linearly correlated by Eq. 10. Development of a trend for propane BIPs used three-phase data given in Gregorowicz et al. (1993b), in addition to the UCEP data mentioned previously, to add an optimized BIP for propane with n-C_{20}. The data by Gregorowicz et al. (1993b) are 12 PT envelopes for 12 different mixtures of ethane, propane, and n-C_{20}. The BIP of ethane with n-C_{20} was calculated with Eq. 10. The T_C, P_C, and ω for n-C_{20} were calculated from Eqs. 1, 2, and 4, respectively. Then, three-phase data were matched by adjusting the propane BIPs with ethane and n-C_{20}. The optimized BIP is 0.017 for ethane/propane and 0.041 for propane/n-C_{20}. Even though three-phase PT envelopes have very-small temperature windows (2.19 K at most), they were successfully matched. **Fig. A-3** shows one such matching. The experimental data for UCEP and LCEP are 316.03 K and 54.59 bar and 315.06 K and 53.33 bar, respectively. The predicted UCEP and LCEP are 315.77 K and 54.40 bar and 314.73 K and 53.00 bar, respectively. The trend of propane BIPs with respect to CN of the heavier *n*-alkane is shown in **Fig. A-4,** which is expressed in Eq. 11. It is evident that the optimized BIPs for n-C_{46} and n-C_{60} do not follow the trend because of the irregularity shown in Fig. A-1.

Development of a trend for methane BIPs required additional three-phase data, because of the scarcity of the UCEP data, such as Hottovy et al. (1981b) for the methane/ethane/n-C_8 system,

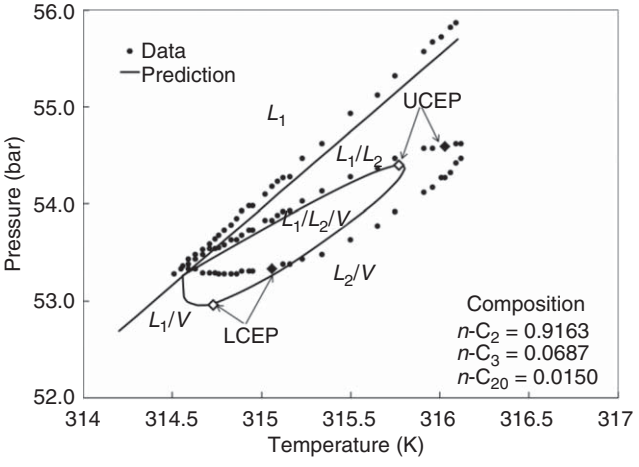

Fig. A-3—Three-phase envelope for a mixture of ethane, propane, and eicosane (Gregorowicz et al. 1993a). Predictions are by use of the PR-EOS with adjustment of propane BIP with eicosane.

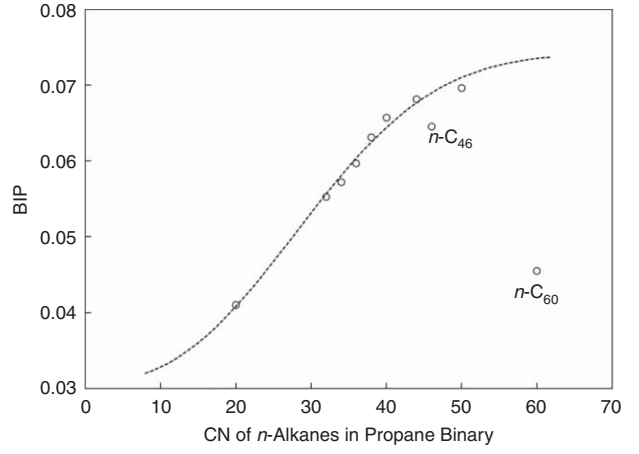

Fig. A-4—Trend of propane BIPs with respect to CN of the heavier *n*-alkane. The curve is given by Eq. 11.

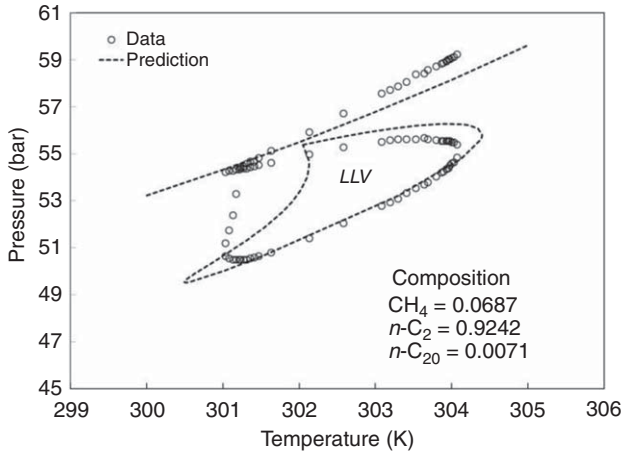

Fig. A-5—Three-phase envelope measured for a mixture of methane, ethane, and eicosane (Gregorowicz et al. 1993b). The predictions are by use of the PR-EOS with the adjusted methane BIP with eicosane, 0.062.

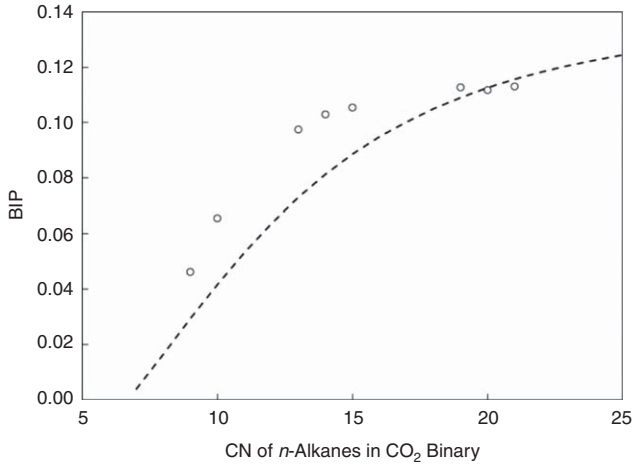

Fig. A-6—Trend of CO_2 BIPs with respect to CN of the heavier *n*-alkane. The curve is calculated from Eq. 8.

Gregorowicz et al. (1993b) for the methane/ethane/n-C_{20} system, and Jangkamolkulchai and Luks (1989) for the methane/ethane/n-C_{22} system. For the system studied by Hottovy et al. (1981b), three-phase composition data at 202.00 K and 48.40 bar, 204.00 K and 50.80 bar, 206.00 K and 54.20 bar, and 210.00 K and 58.80 bar were matched. For the system studied by Gregorowicz et al. (1993b), 11 instances of PT three-phase data were matched. **Fig. A-5** shows one such PT three-phase envelope for 6.87% methane, 92.42% ethane, and 0.71% n-C_{20}. For the system studied by Jangkamolkulchai and Luks (1989), three-phase composition data at 298.50 K and 46.88 bar, 298.50 K and 56.16 bar, 303.50 K and 47.35 bar, and 303.50 K and 52.43 bar were matched. Optimized BIPs for methane/ethane, methane/n-C_8, methane/n-C_{20}, and methane/n-C_{22} are 0.040, 0.048, 0.062, and 0.064, respectively. Eq. 9 gives a correlation for the methane BIPs with CN of the heavier n-alkane.

Three-phase data for the butane binaries and the pentane binaries are unavailable in the literature. It seems that UCEPs were measured for butane with a few n-alkanes (Peters 1994); however, the data are not available in the public domain. In the absence of relevant data, an extrapolation approach was used to develop BIPs of butane and pentane with heavier n-alkanes. For n-alkanes heavier than hexane, BIPs for methane, ethane, and propane were calculated by use of Eqs. 9, 10, and 11, respectively. Then, for each of the heavier n-alkanes, BIPs for methane, ethane, and propane were extrapolated for BIPs for butane and pentane. The resulting correlations are given in Eqs. 12 and 13. These correlations were further validated by three-phase predictions, as shown in the Case Studies section.

BIPs for CO_2 with n-alkanes were optimized by Kato et al. (1981), Lin (1984), and Kordas et al. (1994); however, they did not use three-phase data or CEP data. In this research, therefore, BIPs of CO_2 with n-alkanes were optimized to match the UCEP data for CO_2/n-alkanes, n-C_{13}, n-C_{14}, n-C_{15}, n-C_{19}, n-C_{20}, and n-C_{21} (Hottovy et al. 1981a; Fall and Luks 1985; Fall et al. 1985). To make the trend more reliable, $L = V$ critical-point data for n-C_8, n-C_9, and n-C_{10} (Reamer and Sage 1963; Choi and Yeo 1998) were also used in the BIP optimization. **Fig. A-6** shows that the optimized BIPs demonstrate an increasing trend with increasing CN, but they become nearly constant beyond n-C_{15}. However, higher BIP values were required when matching experimental data for heavy oils for the development of Eqs. 5, 6, and 7. This observation may be because of the effect of oil aromaticity on phase behavior with CO_2, and was considered for the development of Eq. 8.

The n-alkane BIPs developed for the PR-EOS in this research are used for pseudocomponents in this research. Although these BIPs were successful in predicting three-phase behavior in this research, they can be used as initial guesses if BIP adjustment is needed.

Appendix B—Multiphase Slimtube Simulation

The reliability of the new algorithm is tested here by simulating the West Sak oil displacement by enriched gas. This displacement was experimentally shown to exhibit complex three-hydrocarbon-phase behavior. Okuyiga (1992), DeRuiter et al. (1994), and Mohanty et al. (1995) presented slimtube-test data for this oil with seven different injection-gas mixtures, consisting of n-alkanes from C_1 through C_4, at 291.5 K. The seven injection gases were prepared at different levels of methane dilution: 0, 32, 42, 51, 62, 70, and 80 mol% of the methane concentrations. Three hydrocarbon phases were observed for the displacements at the following dilution levels: 32, 42, 51, and 62 mol% of methane. As reproduced in **Fig. B-1,** the oil recovery showed a nonmonotonic trend with respect to methane dilution (Okuyiga 1992).

A consistent set of PVT data is not available in the public domain for characterization of West Sak oil with the new algorithm. Therefore, the molecular weight of West Sak oil, 330 g/mol, is taken from Oil A of DeRuiter et al. (1994). The saturation pressure of the mixture of 29.48% methane and 70.52% West Sak oil at 291.5 K is taken from Oil B of Okuyiga (1992), which is 96.5 bar. Densities of the methane/oil mixture (27.47% methane) at 291.5 K at 70.0 and 96.5 bar are approximated to be 0.915 and 0.919 g/cm^3, respectively, on the basis of Oil A of Okuyiga (1992).

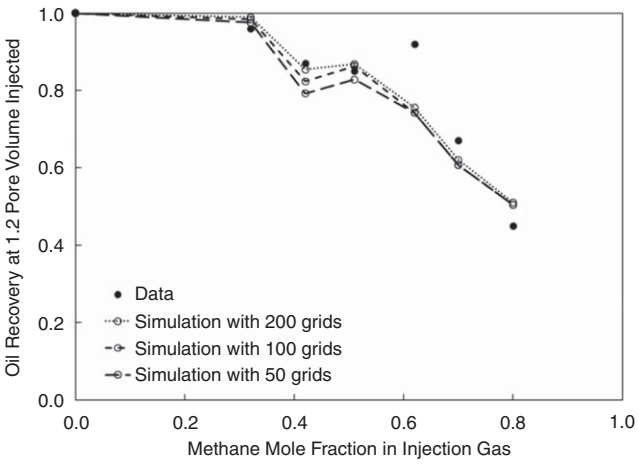

Fig. B-1—Oil recovery for the West Sak oil displacement by enriched gas at 103.42 bar and 291.5 K. The data were taken from Okuyiga (1992).

Number of grids	50/100/200
Width	0.015 ft
Length	0.600 ft
Thickness	0.015 ft
Horizontal permeability	5,000 md
Porosity	0.35
Residual water saturation	0.00
Residual oil saturation	0.20
Residual second-liquid saturation	0.10
Residual gas saturation	0.30
Oil endpoint relative permeability	0.80
Second endpoint relative permeability	1.0
Gas endpoint relative permeability	1.0
Oil relative permeability exponent	4.50
Second-liquid relative permeability exponent	1.50
Gas relative permeability exponent	3.50

Table B-1—Parameters used in slimtube simulation.

The compositional characterization of the oil is dependent on the chi-squared distribution with the degree of freedom of 12. The regressed values for k and β (see the Multiphase-Fluid Characterization section) are 4258 and 1.8269, respectively.

The viscosity of the methane/oil mixture (27.92% methane) is approximated to be 99 cp at 96.5 bar and 291.5 K (Oil C of Okuyiga 1992). The viscosity is matched by adjusting critical volumes with the viscosity model of Lohrenz et al. (1964).

Table B-1 summarizes other parameters for slimtube simulation. Relative permeability data for three hydrocarbon phases are not available (Mohanty et al. 1995). Therefore, the conventional Corey (1954) model is used for estimation of relative permeabilities for three hydrocarbon phases. Oil recoveries for two immiscible displacements at the methane concentrations of 70 and 80 mol% have been used to determine the relative permeability parameters.

Simulations are performed with UTCOMP (Chang 1990; Chang et al. 1990), which is a multiphase multicomponent EOS compositional simulator developed at the University of Texas at Austin. Oil displacements by seven injection gases with the methane concentrations of 0, 32, 42, 51, 62, 70, and 80 mol% (Okuyiga 1992) are simulated at 103.42 bar and 291.50 K. Three different numbers of gridblocks—50, 100, and 200—are used to observe the sensitivity of oil-recovery simulations to numerical dispersion.

Without methane dilution (i.e., 0% methane in the injection gas), the displacement is simulated to be first-contact miscible. A large three-hydrocarbon-phase region is present in the simulations with the methane concentrations of 32, 42, 51, and 62%. The three-hydrocarbon-phase region becomes small at 70% methane, and only two phases are simulated in the oil displacement at 80% methane.

The trend of oil recovery at 1.2 pore volumes injected with respect to methane dilution is presented in Fig. B-1. Fig. B-1 indicates that the miscibility levels of oil displacements are reasonably represented by the EOS model developed. Although the oil recovery simulated at 62% methane deviates from the experimental data, Fig. B-1 shows a nonmonotonic trend of oil recovery, which is caused by three-hydrocarbon-phase flow (Okuno and Xu 2014b). The simulation results are affected also by uncertainties in relative permeability, viscosity, and density. However, it is shown that use of the new algorithm for multiphase fluid characterization results in reasonable representation of varying miscibility level in the three-hydrocarbon-phase displacement.

Ashutosh Kumar worked with GAIL (India) Limited for 10 years as a petroleum engineer. His research interests include enhanced oil recovery and thermodynamic modeling of multiphase behavior. Kumar is a member of SPE. He holds a bachelor's degree from the Indian School of Mines, a master's degree from the University of Regina, and a PhD degree from the University of Alberta, all in petroleum engineering.

Ryosuke Okuno is an assistant professor in the Department of Petroleum and Geosystems Engineering at the University of Texas at Austin. Before his current position, he served as an assistant professor of petroleum engineering in the Department of Civil and Environmental Engineering at the University of Alberta from 2010 to 2015. Okuno also has 7 years of industrial experience as a reservoir engineer with Japan Petroleum Exploration Company Limited and is a registered professional engineer in Alberta, Canada. His research and teaching interests include enhanced oil recovery, thermal oil recovery, oil-displacement theory, numerical reservoir simulation, thermodynamics, multiphase behavior, and applied mathematics. Okuno is a member of SPE, a recipient of the 2012 SPE Petroleum Engineering Junior Faculty Research Initiation Award, and an associate editor for *SPE Journal and Journal of Natural Gas Science & Engineering*. He holds bachelor's and master's degrees in geosystem engineering from the University of Tokyo, and a PhD degree in petroleum engineering from the University of Texas at Austin.